2003

Fundamentals and process modeling of supersonically induced mechanical alloy technology (SIMAT(TM)) for engine production.

Evgeny. Leshchinsky
University of Windsor

Fundamentals and Process Modeling of Supersonically Induced Mechanical Alloy Technology (SIMAT™) for Engine Production.

by

Evgeny Leshchinsky

A Thesis
Submitted to the Faculty of Graduate Studies and Research
through the Department of Industrial and Manufacturing
System Engineering
in Partial Fulfillment of the Requirement for
the Degree of Master of Applied Science
at the University of Windsor.

Windsor, Ontario, Canada

2003

Your file Votre référence
ISBN: 0-612-82872-7
Our file Notre référence
ISBN: 0-612-82872-7

The University of Windsor requires the signatures of all persons using or photocopying this thesis. Please sign below and give an address and the date.

I hereby declare that I am the sole author of this thesis. I authorize the University of Windsor to lend this thesis to other institutions or individuals for the purpose of scholarly research.

Evgeny Leshchinsky

I further authorize the University of Windsor to reproduce this thesis by photocopying or by other means, in total or in part, at the request of other institutions or individuals for the purpose of scholarly research.

Evgeny Leshchinsky

ABSTRACT

Conventional Metal Powder Coatings, designed to obtain anti-corrosive, wear and thermal resistant properties, are studied and their properties are analyzed. The capabilities of the Supersonically Induced Mechanical Alloy Technology are investigated with the purpose to enhance the surface strength and durability, simplify the deposition procedure and increase service time. A new spray deposition process is shown and compared with other different methods of Metal Powder Coating deposition. A new method is developed that is less expensive and operates with similar load mechanisms on powder particles. High strain rate deformation can be easily studied by special powder compaction. In this method, the powder is loaded into a die with skewed punches and deformed under high strain rates. The bonding conditions of powder particles are shown to be similar to those obtained in SIMAT process. The composite microstructure, mechanical properties and special characteristics of the coatings delivered using Supersonically Induced Mechanical Alloy Technology are investigated and described. The methodology used to analyze the mechanical properties of coatings is explained. Experimental results using the ultrasonic scanning systems are presented.

DEDICATION

To My Parents

ACKNOWLEDGMENTS

The work presented in this thesis could not been possible without support of many people.

I wish to express my sincere gratitude to my research supervisors Dr. M. Wang and Dr. R. Maev for their continuous support and help. The successful completion of this thesis depended on their useful ideas and guidance.

I wish to express my appreciation to Dr. Q. Zhang and Dr. J. Sokolowski for their consideration to be Department Readers and members of the Defense Committee. Their assistance, advice and remarks are greatly appreciated.

My special thanks extend to our department coordinators Ms. Sarah Beneteau, Ms. Emily Schmidt, Ms. Jacquie Mummery and Ms. Sharon Horne for their attention and help.

I wish to express my gratitude to Mr. Louis Beaudry, Mr. Erik Clausen and Mr. Robert Clark for their efforts and practical contribution to this work.

I would like to thank my parents for their love, support and encouragement during the entire period of my education.

Finally, I would like to thank my wife Elena Leshchinsky, who patiently endured difficult times, and her invaluable support has contributed to the completion of this dissertation.

TABLE OF CONTENTS

Chapter 1

Introduction

1.1 General

The idea and the early physical principles of low-temperature *Supersonically Induced Mechanical Alloy Technology (SIMAT™)* also known as Gas-Dynamic Spray, were initiated about 1985 [4]. The early investigation work was completed by the Russian Academy of Sciences and for the last four years has been continued in North America.

The main benefit of this technology is to eliminate high-temperature two-phase flows, which are the major shortcomings inherent in all thermal spraying techniques. In all known techniques such as flame spraying, high velocity oxy-fuel spraying, arc-discharge spraying, plasma spraying and detonation coating, the formation of coatings is a result of interaction between completely or partly melted sprayed particles with the substrate [6].

SIMAT™ is a low temperature process and does not create the high-temperature environment of the conventional spraying processes that affects both the substrate (especially thermally non-stable substrates) and the deposited coatings. The high-temperature processing can cause thermal deformation of substrates, deterioration of material properties and peeling or flaking of coatings. All these disadvantages are eliminated in the new SIMAT™ method. In addition, traditional methods require expensive and technically sophisticated high temperature devices (e.g. plasmatrons, burners, detonation guns, etc.) that considerably narrow the possible applications of the coating deposition with special difficulties encountered in machine workshop conditions. At the same time, the feasibility of application of SIMAT™ equipment in a workshop is evident.

The emerging SIMAT™ technology, now in development, has the potential to revolutionize the thermal spray industry by intrinsically changing thermal spray processes and adding new flexibility to powder material deposition technology.

1.2 Statement of the problem

At the present time the Metal Powder Coating industry uses a number of Thermal Powder Spray techniques that allow depositing a broad variety of different metal powders including specially designated for processed alloys. It became possible due to the extended investigation work in the area of Thermal Powder Spray and complete understanding of all concurrent powdered metal forming processes taking place during the deposition. The capacious database of Thermal Powder Spray knowledge allows us to select a coating deposition process and its parameters for each particular case avoiding time-consuming tests and able to predict coating properties depending on the metal powder being used.

However, unlike the Thermal Powder Spray, the new Gas-Dynamic Spray process is not completely studied and fully understood especially from the point of view of metallography. The lack of ruling factors that influence the SIMAT™ coating formation hinders the material selection, makes predicting coating properties impossible and constraints further development of composite powders, which are specifically suited for SIMAT™ process. All together, these troubles make SIMAT™ technology unable to respond adequately to customer requirements, unable to compete with extensively developed Thermal Powder Spray, which eventually delayed introduction of this technology into the real business and narrow the area of its application.

There are several problems related to an investigation of the mechanism of coating formation for SIMAT™ technology. First, it is a complex inhomogeneous powder mix that does not represent a single alloy, rather it is a so-called mechanical alloy or a mix of

different powders that does not have certain stable mechanical and metallographic characteristics. They vary from compound of powders, their chemical composition and relative proportions. As a result, for mixes with similar compounds we generally receive different types of coatings with different properties just because of their different component proportions. The second significant problem associated with SIMAT™ study is determination of the gas flow parameters. Since the SIMAT™ uses a kinetic approach for metal particle deposition, it is very important to know the velocities of the propellant gas and metal particles in its medium [3]. However, it was discovered that to compute real velocities of the gas and metal particles is as difficult as to measure them in a real experiment. One part of the problem arises from difficulties to calculate the flow parameters because of the great losses occurring in a nozzle with a small cross-section size. Besides that, the injection flow of a metal powder stream fed into the nozzle additionally complicates the computation. Measuring the pressure drop occurring in the nozzle during the process gave us a rough idea about the gas velocities and nothing about the real metal particle velocities that we are interested in. Meantime, even for gas velocities we received scattered results ranging from 300 to 1200 m/s that do not really reflect any correlation between the flow parameters and the resulting coating bonding properties.

Thus, since coating bonding properties depend mostly on the powder mix compound and the gas flow parameters during the deposition, then our goal is to find the proper characteristics for powder mix and gas flow parameters that influence the bonding mechanism of the coating formation. If we knew this interdependence, then we would be able to obtain desirable coatings, predict their properties, facilitate metal powder selection and optimize the process parameters.

1.3 Objectives and Plan of the Research

Research into SIMAT™ technology involves the development of a methodology for study of SIMAT™ coatings, study of their mechanical properties using special equipment for mechanical tests and coating layer structure investigation using acoustic microscopy. Important research areas include the determination of the criteria for powder selection for certain type of coatings and methods for control of the gas flow parameters.

In order to successfully accomplish all these tasks and completely clarify all the phenomena occurring during the coating deposition process and the ultimate bonding formation, an introduction into the metal powder compaction principles is considered to be crucial. The basic principles of the powder compaction processes characterization are supposed to be applied to the selected experimental powder mixtures pursuing an attempt to predict the properties of the experimental coatings and to describe the bonding mechanism of their formation.

The completion of both theoretical interpretation and the experimental analysis will result in creating a series of summary charts reflecting the interdependence between coating properties versus all theoretical and experimental characteristics of the investigated coatings and deposition process parameters.

Regarding the practical application of the new emerged SIMAT™ technology and the assessment of its industrial potentials the analysis of the existing Metal Powder Coating market are supposed to be provided. In order to get a complete image of the available on the market competitive technologies, their descriptions, comparison characteristics and their corresponded advantages and disadvantages become the subjects for an additional investigation.

In the conclusion of this research the feedback of the already implemented SIMAT™ applications will be discussed, the benefits of those innovations are stated and a new scope for SIMAT™ introduction will be outlined and substantiated.

1.4 Formal Presentation

The main objective of the proposed thesis is determination of the mechanism for SIMAT™ coatings formation and its interpretation from the point of view of solid-state Physics. If we knew the SIMAT™ key factors influencing the coating formation and a model of metal powder particles interaction, then we would be able to simulate the coating layer structure and to predict the major coating properties.

Therefore, the proposed thesis starts with the description of the SIMAT™ method and a schematic representation of the equipment being used. Analysis of already developed SIMAT™ coating and their major properties will be described. Further this information will be used as a basis for creating the relation between SIMAT™ parameters and the properties of the obtained coatings, as well as for investigating a coating formation mechanism and creating a basic theoretical idea about how this mechanism works.

Therefore, it is considered to be essential for the reader to comprehend the basic principles of the Solid-State Physics applied in our case in order to describe the mechanism of metal powder compaction process that eventually makes a formation of a fully dense SIMAT™ coating possible.

A design of an experiment for evaluation of material mechanical properties will be presented. In our case this will allow us to use the standard mechanical tests for powdered materials with thin SIMAT™ coatings. The procedure is intended to simplify a powder material selection for certain types of coatings, as well as to facilitate evaluation of major properties of prospective coatings at minimum costs and the highest accuracy.

In order to get a better idea about the potentials of SIMAT™ technology and its apparent benefits for industrial use, it is considered to be necessary to provide comparative

analysis of the new SIMAT™ technology with conventional Thermal Metal Powder Spray techniques.

The first North-American experience of SIMAT™ application for engine block thermal cracks and cylinder head corrosion pits repair will be described. A prospective scope for SIMAT™ potential applications will be outlined.

Chapter 2

Literature Review of Existing Metal Powder Spray Deposition Techniques

2.1 Historic Background

The metal spraying industry has its beginnings early in the 20th century when Dr. M.U. Schoop of Zurich, Switzerland, developed the first process for spraying metal and, subsequently, the first equipment to spray metal in wire form. The early commercial applications for the "Schoop Process"or "metallizing" took place in Germany, and later in France. Schoop subsequently sold his rights to a German firm known as Metallizator. It was this firm that made and sold spray units in Europe, England and the United States beginning in the early 1920"s. Among the early U.S. companies to adopt the technology were Metal Coatings Company and Metalweld of Philadelphia and Metallizing Company of Los Angeles. Early applications included the coating of railroad tank cars, U.S. Navy ship tanks, coal barges and the spraying of the emergency gates for the Panama Canal.

Applications for industrial plants accelerated during the "Great Depression," and during this decade the greatest push for what was then known as "flame spraying" occurred. Four entrepreneurs – Larry Kunkler, Rea Axline, Charles Boyden, Sr. and Charles Stipp from the Metallizing Company of America – were largely responsible for pushing metallizing into the American industrial scene.

With the advent of World War II, the American thermal spray industry went into high gear with the members of the association playing a key role in providing the

"metallizing" desperately needed for replacement parts for industrial equipment. Walter Meyer and Tom Lufkin of Tranter Manufacturing Company worked with the Army in the China-Burma-India theater; Knowles Smith of Dix Engineering Company worked with the Navy. By the end of the war, "metallizing" was firmly established as a major industrial process. Applications included large elevated water tanks, tuna fishing boats, chemical industry tanks and tank cars, capacitor castings and pipe.

In response to an increasingly sophisticated market, International Thermal Spray Association (ITSA) drew up industry specifications for the application of corrosion-resistant coatings and spelled out the methods of inspection. These specifications were distributed to engineering firms, designers, and educational institutions throughout the world and resulted in increased business opportunities for the entire metallizing industry. The advent of fusible alloys, flame spraying of ceramics and plasma spraying were soon to follow.

ITSA members were also important contributing authors and researchers for the manual of *Thermal Spraying – Practice and Theory Application* [1]. Published in 1985, this was the first definitive work on thermal spray produced in the United States.

2.2 Metal Powder Spray Competitive Technologies

The most commonly used method for Metal Powder Deposition is Thermal Spray, which is relatively simple and consists of the following stages :

1. Melting the metal at the gun
2. Spraying the liquid metal onto the prepared substrate by means of compressed air
3. Molten particles are projected onto the cleaned substrate

Thermal Metal Powder Spray currently is represented by five major metal powder deposition techniques:

1. Flame Metal Powder Spraying
2. High Velocity Oxygen Fuel - HVOF - Thermal Spray Coating Process
3. Electric Discharge Arc Metal Powder Spraying
4. Plasma Metal Powder Spraying
5. Detonation Metal Powder Thermal Spray

2.2.1 Flame Metal Powder Spraying

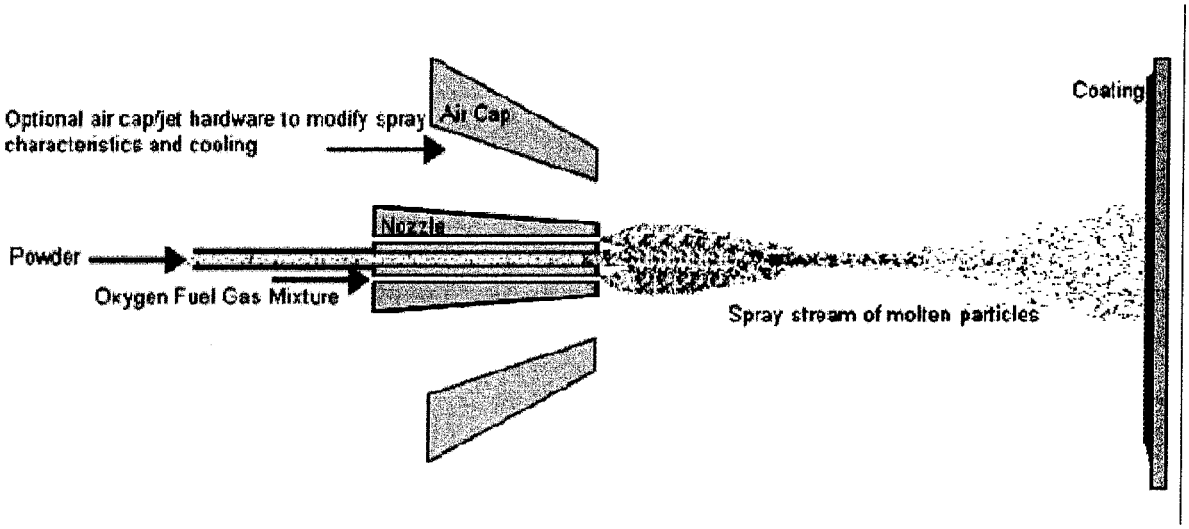

Figure 2-1. Schematic Diagram of Flame Metal Powder Spraying

The Flame Spraying Process (also known as Low Velocity Oxygen Fuel Process) is basically a spraying of molten material onto a surface to provide a coating. Material in

powder form is melted in a flame (oxy-acetylene or hydrogen most common) to form a fine spray. When the spray contacts the prepared surface of a substrate material, the fine molten droplets rapidly solidify forming a coating.

The main advantage of this Flame Spraying Process is a wide range of materials that can be easily processed into powder form giving a larger choice of coatings. The flame spraying process is only limited by materials with higher melting temperatures than the flame can provide or if the material decomposes on heating.

2.2.2 High Velocity Oxygen Fuel - HVOF - Thermal Spray Coating Process

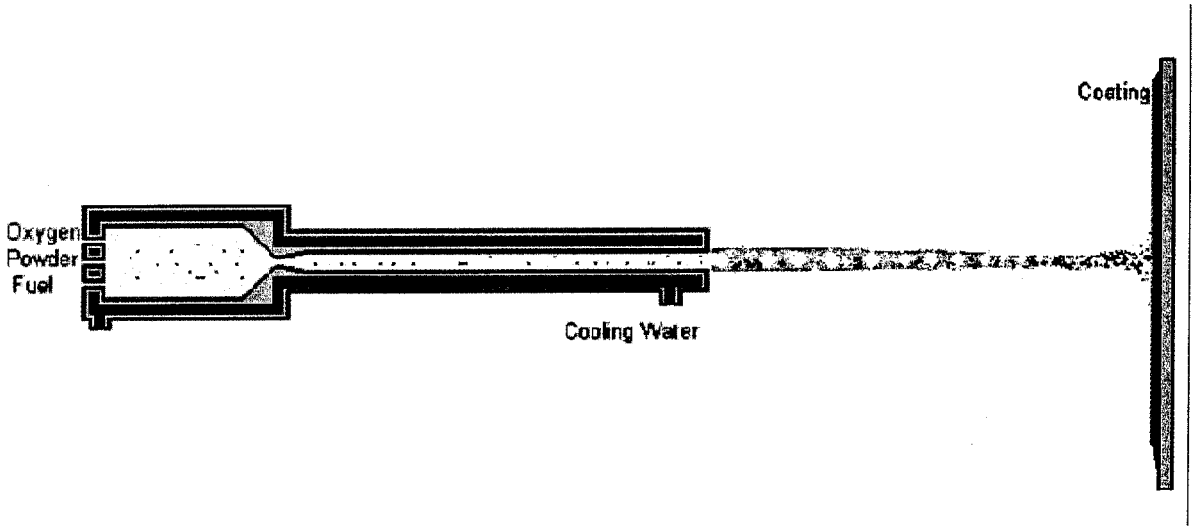

Figure 2-2. Schematic Diagram of HVOF Powder Spraying

The HVOF (High Velocity Oxygen Fuel) Thermal Spray Process is basically the same as the Flame Powder spray process (LVOF) except that this process has been developed to produce extremely high spray velocity. There are a number of HVOF guns which use different methods to achieve high velocity spraying. One method is basically a high pressure water cooled combustion chamber and long nozzle. Fuel (kerosene, acetylene, propylene and hydrogen) and oxygen are fed into the chamber, combustion produces a hot high pressure flame which is forced down a nozzle increasing its velocity. Powder

may be fed axially into the combustion chamber under high pressure or fed through the side of Laval type nozzle where the pressure is lower.

HVOF coatings are used in applications requiring the highest density and strength not found in most other thermal spray processes. Coatings are very dense, strong and show low residual tensile stress or in some cases compressive stress, which enable very much thicker coatings to be applied than previously possible with the other processes. The very high kinetic energy of particles striking the substrate surface do not require the particles to be fully molten to form high quality coatings. This is certainly an advantage for the Carbide Cermet type coatings and is where this process really excels.

2.2.3 Electric Discharge Arc Metal Powder Spraying

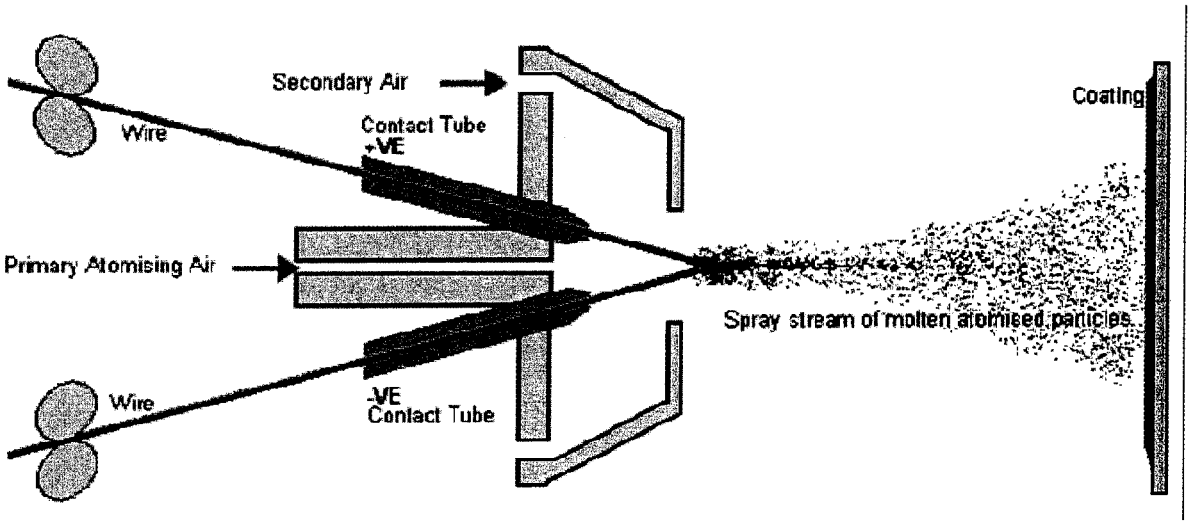

Figure 2-3. Schematic Diagram of Electric Arc Spraying

In the Arc Spraying Process a pair of electrically conductive wires are melted by means of an electric arc. The molten material is atomised by compressed air and propelled towards the substrate surface. The impacting molten particles on the substrate rapidly

solidify to form a coating. Arc spray coatings are normally denser and stronger than their equivalent combustion spray coatings. Low running costs, high spray rates and efficiency make it a good tool for spraying large areas and high production rates.

Disadvantages of the arc spraying process are that only electrically conductive wires can be sprayed and if substrate preheating is required, a separate heating source is needed.

The main applications of arc spraying are anti-corrosion coatings of zinc and aluminium and machine element work on large components.

2.2.4 Plasma Metal Powder Spraying

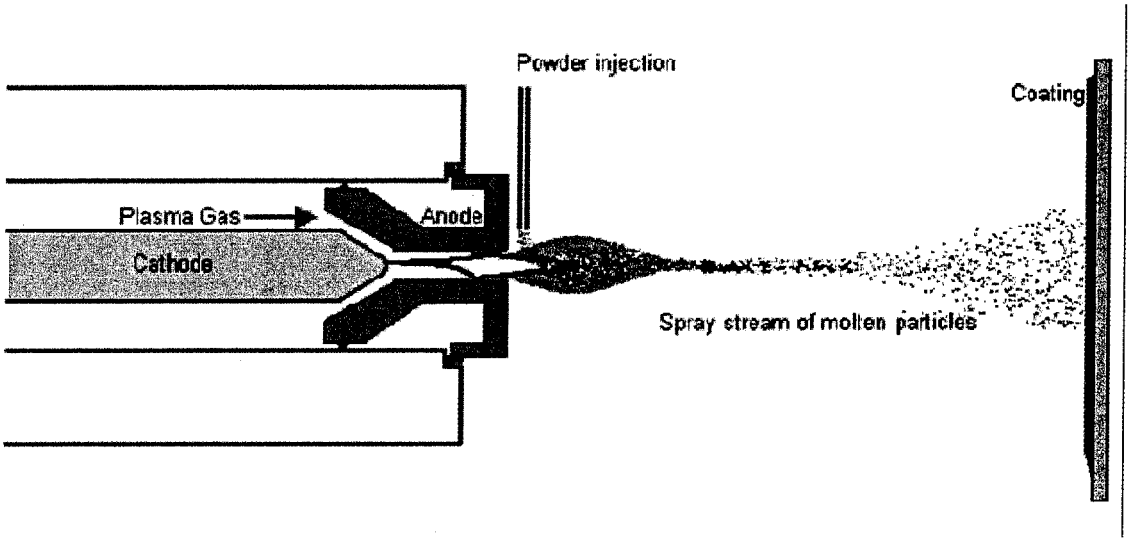

Figure 2-4. Schematic Diagram of Plasma Spraying

The Plasma Spray Process is basically the spraying of molten or heat softened material onto a surface to provide a coating. Material in the form of powder is injected into a very high temperature plasma flame, where it is rapidly heated and accelerated to a high velocity. The hot material impacts on the substrate surface and rapidly cools forming a coating. The plasma gun comprises a copper anode and tungsten cathode, both of which are water cooled. Plasma gas (argon, nitrogen, hydrogen, helium) flows around the cathode and through the anode which is shaped as a constricting nozzle. The plasma is

initiated by a high voltage discharge which causes localised ionisation and a conductive path for a DC arc to form between cathode and anode. The resistance heating from the arc causes the gas to reach extreme temperatures, dissociate and ionise to form a plasma. Powder is fed into the plasma flame most commonly via an external powder port mounted near the anode nozzle exit. The powder is so rapidly heated and accelerated that spray distances can be in the order of 25 to 150 mm.

Plasma spraying has the advantage that it can spray very high melting point materials such as refractory metals like tungsten and ceramics like zirconia unlike combustion processes. Plasma sprayed coatings are generally much denser, stronger and cleaner than the other thermal spray processes with the exception of HVOF and detonation processes. Plasma spray coatings probably account for the widest range of thermal spray coatings and applications and makes this process the most versatile.

Disadvantages of the plasma process are relative high cost and complexity of process.

2.2.5 Detonation Metal Powder Thermal Spray

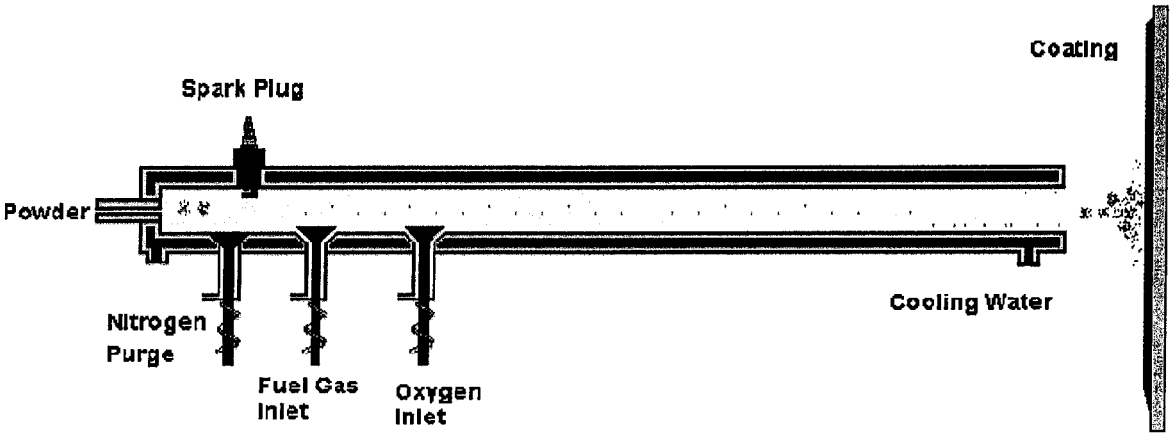

Figure 2-5. Schematic Diagram of Detonation Spraying

The Detonation gun basically consists of a long water cooled barrel with inlet valves for gases and powder. Oxygen and fuel (mostly common acetylene) is fed into the barrel along with a charge of powder. A spark is used to ignite the gas mixture and the resulting detonation heats and accelerates the powder to supersonic velocity down the barrel. A pulse of nitrogen is used to purge the barrel after each detonation. This process is repeated many times a second. The high kinetic energy of the hot powder particles released during an impact with the substrate result in a build up of a very dense and strong coating.

2.2.6 Direct Metal Powder Deposition - DMD

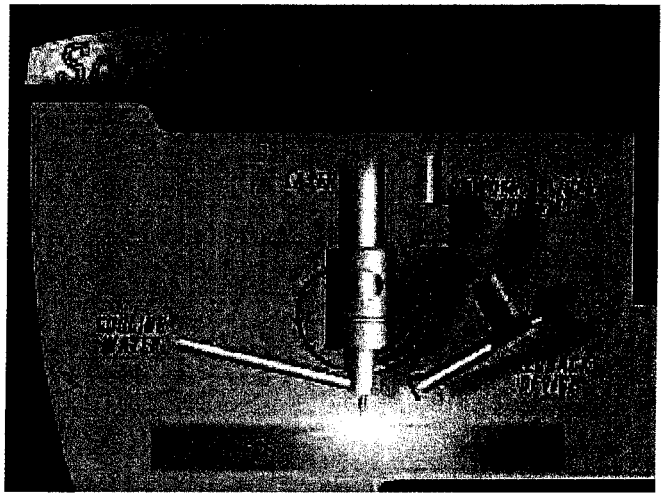

Figure 2-6. Schematic Diagram of DMD Process

DMD™ is a process that fabricates fully dense metal "from the ground up" using powdered metal and a focused laser. Materials deposited via thermal spray processes often times fail due to high levels of porosity or the presence of a heat-affected zone imposed at the interface. The DMD process provides the ability to develop a strong metallurgical bond between dissimilar materials without associated porosity and

significant thermal shock on a substrate. There is a laser heating and melting a small surface spot and powder supplied by small portions to be fused up to a preheated area. The process is conducted in the protecting gas environment and CNC administrated.

Disadvantages are extremely high costs, immobility of the equipment, impossible deposition of ceramic materials.

2.3 Common Features of Thermal Spray Coatings

2.3.1 Grain Structure of Thermal Spray Coatings.

A common feature of all thermal spray coatings is their lamellar grain structure resulting from the rapid solidification of small globules, flattened from striking a cold surface at high velocities (Fig. 2-7).

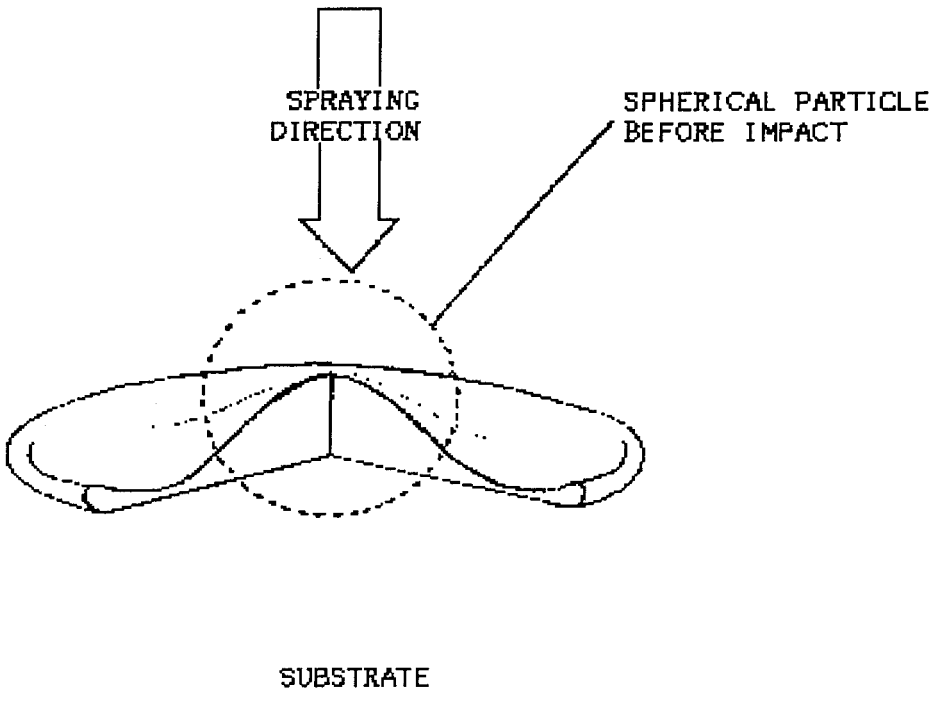

Figure 2-7. Schematic diagram of thermally sprayed spherical particle impinged onto a flat substrate

2.3.2 Side effects of Thermal Spray Processes

Due to the Thermal Spray nature it inevitably produces voids, oxides, not melted inclusions. High cooling rates or super cooling (10^6 Ks^{-1}) of particles can cause the formation of unusual amorphous (glassy metals) microcrystaline and metastable phases not normally found in wrought or cast materials. That is evident in the coating microstructure as oxide inclusions outlining the grain or particle boundaries (Fig. 2-8).

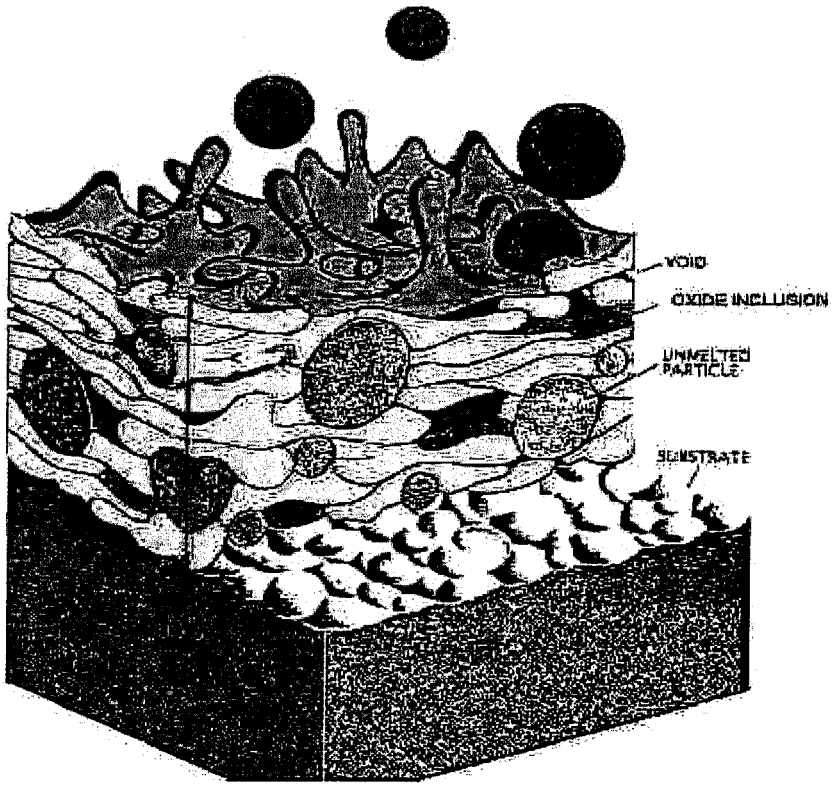

Figure 2-8. Schematic diagram of Thermal Spray Metal Coating

2.3.3 Anisotropy of Thermal Spray Coatings

Coatings show lamellar or flattened grains appearing to flow parallel to the substrate. The structure is not isotropic, with physical properties being different parallel to substrate (longitudinal) than across the coating thickness (transverse). Strength in the longitudinal direction can be 5 to 10 times that of the transverse direction (Fig. 2-9).

Figure 2-9. Microstructure of Nickel Chromium thermally sprayed coating. The lamellar structure is interspersed with oxide inclusions and porosity

2.3.4 Porosity

All conventionally thermally sprayed coatings contain from 0.25% to 50% of porosity. Porosity is caused by:

- Low impact energy (unmelted particles / low velocity)
- Shadowing effects (unmelted particles / spray angle)
- Shrinkage and stress relieve effects

2.3.5 Typical Failure of Thermal Spray Coatings

Cooling and solidification of most materials is accompanied by contraction or shrinkage. As particles strike they rapidly cool and solidify. This generates a tensile stress within the particle and a compressive stress within the surface of the substrate. As the coating is built up, so are the tensile stresses in the coating. With a lot of coatings a thickness will be reached where the tensile stresses will exceed that of the bond strength or cohesive strength and coating failure will occur (Fig. 2-10).

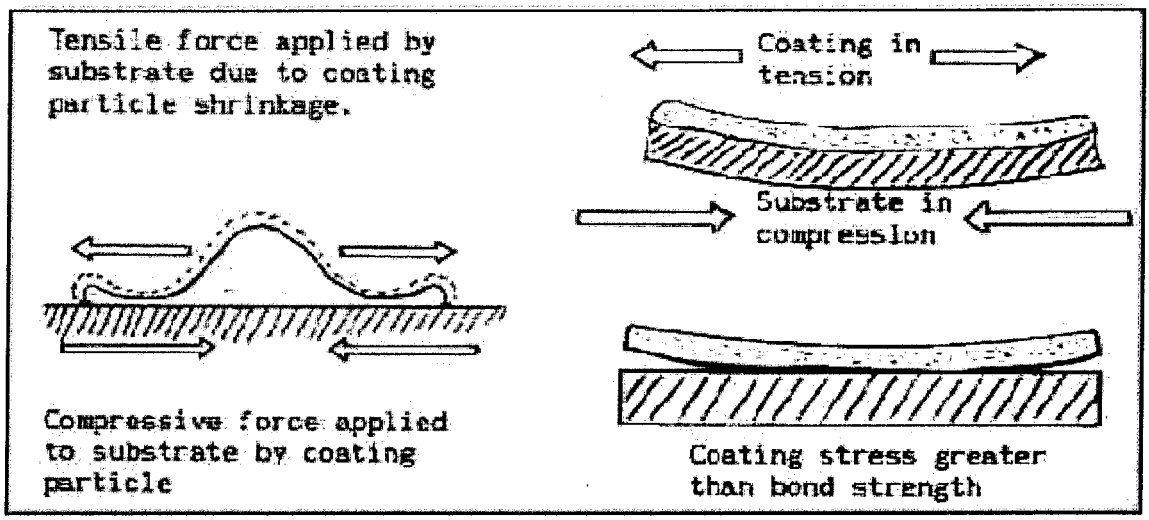

Figure 2-10. Shrinkage and Lamination nature of Thermal Spray Coatings

The above interactions can make the coatings very different from their starting materials chemically and physically.

In order to overcome all known shortcomings inherent in the Thermal Spray Coatings a new cold type of Metal Powder Deposition has been developed. Cold Spray is an exciting new spray technology that has the potential to overcome limitations of more traditional

thermal spray processes for some important commercial applications. With this emerging technology, it is possible for the first time to rapidly deposit thin or very thick layers from millimeters to centimeters of a wide range of metals, and even some composite materials, without melting or vaporization, at or near room temperature, in an ambient air environment.

Chapter 3

SIMAT™ Method Outline

3.1 Early Development of SIMAT™ Process

Cold Spray, which was the predecessor of SIMAT™ process, was first demonstrated in the mid-1980s by Dr. Anatolii Papyrin and colleagues at the Institute of Theoretical and Applied Mechanics (Russian Academy of Sciences). At that time, they demonstrated a material deposition process based on the use of 1- to 50-μm solid metal particles introduced into a gas stream accelerated to supersonic velocities. Research in the U.S. began in 1994 at the National Center for Manufacturing Sciences, which sponsored a technology demonstration program by Dr. Papyrin. In 1995, Ktech and Sandia National Laboratories (SNL) designed and installed a cold spray system at SNL to study the process, and that work continues today[3].

Both Cold Spray and SIMAT™ method for producing thin to very thick deposits of various metals and metal-ceramic mixtures are based on a particle kinetic approach. Solid particles in the size range of 10 to 100 microns are introduced by means of a powder feeder into the high-pressure chamber of a converging-diverging (de Laval) nozzle where they are accelerated into a supersonic stream (ranging from 300 to 1200 m/s) by the propellant gas, which has been electrically preheated prior to introduction into the nozzle (Figure 3.1). These high velocity relatively cold particles are projected on to a work piece. There is no combustion process or electrical discharge in the spray device itself thus powder material retains original characteristics.

A unique attribute to this spraying technique is its ability to generate a wide range of deposited layers thickness ranging from tens of microns up to as much as centimeters. In this regard, the process extends beyond the concept of "coatings" of substrates and includes the capability of material build-up, and developing three-dimensional structures.

The powder material to be deposited can be selected from the groups consisting of metals, alloys, ceramics and glasses.

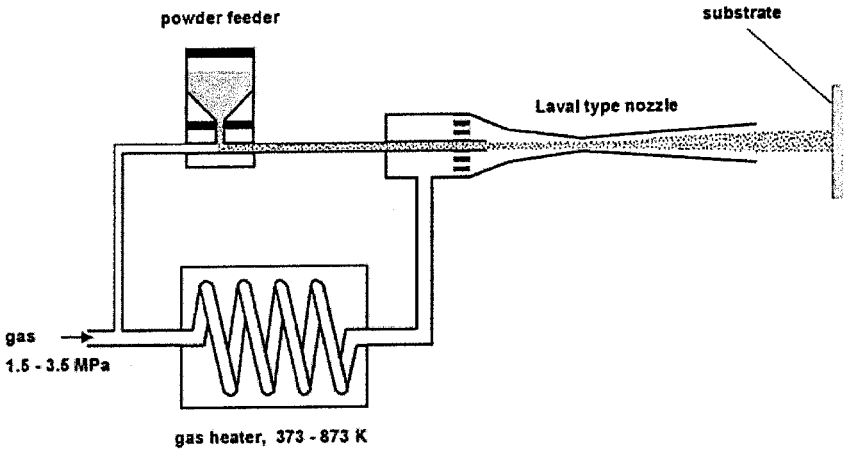

Figure 3.1 Schematic Diagram of Cold Spraying apparatus from Institute of Theoretical and Applied Mechanics of Russian Academy of Sciences

The essential modification of Cold Gas-Dynamic Spray Technology is being made by Prof. Roman Maev with co-workers [4] from 1996. The new SIMAT Gas-Dynamic Spray process was developed on the base of pressure less powder feed method, spray parameters optimization and applying new powder compositions.

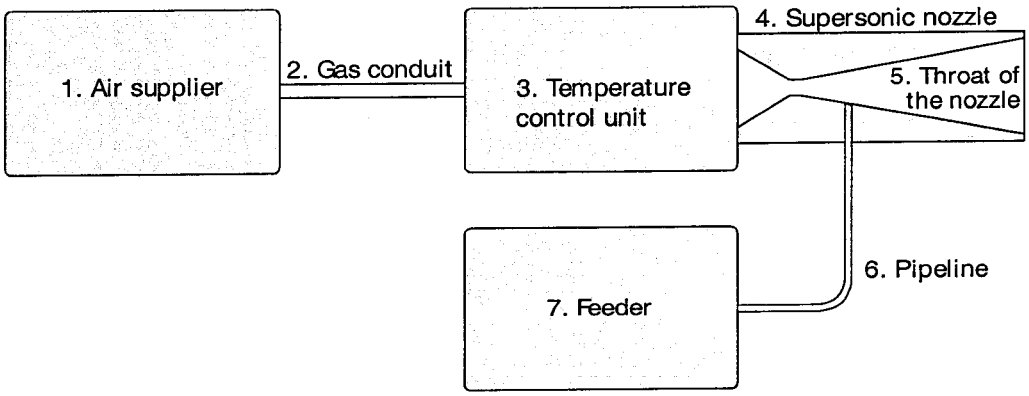

Figure 3.2 Schematic Diagram of the spraying apparatus for SIMAT™ technology

The device for implementing the SIMAT™ technology is shown on Figure 3.2. Compressed air from the compressed air source (1) through the gas conduit (2) is supplied into the temperature control unit (3), where it undergoes heating to required temperature. Heated air enters directly the supersonic nozzle (4), where it is accelerated to the velocity up to several hundreds m/s. The powder material from the powder-hopper (7) through the pipe-line (6) is delivered into supersonic part of the nozzle (well down stream of the maximum nozzle restriction or throat). The nozzle pressure at the point where powder material is entering the nozzle is below atmospheric and provides efficient suction of the powder from the powder-hopper.

The presented device design favorably compares to existing model analogs, and essentially increase operational stability of the apparatus due to the prevention of wear at the nozzle throat. Because powder does not pass through the nozzle, erosion problems are eliminated. Since there are no changes in the nozzle working condition, the nozzle unit and the entire device became more stable, reproducible and reliable.

3.2 SIMAT™ Benefits

3.2.1 Coating Strucutre

High cooling rates or super cooling (10^6 Ks^{-1}) of particles inherent in Thermal Spray can cause the formation of unusual amorphous (glassy metals) microcrystaline and metastable phases not normally found in SIMAT™ coatings.

Chemical interactions occur during Thermal Spraying, notably oxidation. Metallic particles oxidize over their surface forming an oxide shell. This is evident in the Thermal Coating microstructure as oxide inclusions outlining the grain or particle boundaries impeding stromg bonding formation. Beside that, oxides in coatings can be detrimental towards corrosion, strength and machinability. This drawback is eliminated in SIMAT™

completely with exception for metals oxidizing at normal ambient conditions (like Aluminim).

Thermal Coatings show lamellar or flattened grains appearing to flow parallel to the substrate. The structure is not isotropic, with physical properties being different parallel to substrate (longitudinal) than across the coating thickness (transverse). Strength in the longitudinal direction can be from 5 to 10 times less that of the transverse direction. Unlike Thermal Spraing SIMAT™ produces materials with structurture that can be rendered rather like isotropic then anisotropic and indifference of coating properties in longitudinal and transverse directions is not significant.

3.2.2 Bonding

The bonding mechanisms at the coating - substrate interface and between the particles making up the coating is an area, which in many cases is still subject to speculation. It generally suffices to state that both mechanical interlocking and diffusion bonding occur in Thermal Spraying and SIMAT™ processes. Factors affecting bonding and subsequent build up of the coating in both cases are:

- Cleanliness
- Surface area
- Surface topography or profile
- Temperature (thermal energy)
- Time (reaction rates and cooling rates etc.)
- Velocity (kinetic energy)
- Physical and chemical properties of initial materials
- Physical and chemical reactions

However, SIMAT™ is less sensitive to surface cleanliness, surface area, cooling rates and chemical reactions during the deposition process.

3.2.3 Porosity

This is present in most thermally sprayed coatings (except post heat treated coatings or fused coatings). From 10 to 25% porosity is normal but can be further manipulated by changes in process and materials. Porosity of the Thermal Spray coatings is detrimental with respect to:

- Corrosion - (sealing of coatings advised)
- Machined finish
- Strength, micro hardness and wear characteristics.

SIMAT™ coatings avoid these complications providing high density (up to 2%) deposited materials.

3.2.4 Surface Texture

Generally the sprayed surfaces are rough and textured. Many coatings have high friction surfaces as-sprayed and this property is made use of in many applications (rolling road drum surfaces for brake testing). Some plasma sprayed ceramic coatings produce smooth but textured coatings important in the textile industry. Other applications make use of the abrasive nature of some coating surfaces. Both SIMAT™ and thermally sprayed coatings do not provide bright high finish coatings without finishing like that of electroplated deposits.

3.2.5 Strength

Coatings generally have poor strength, ductility and impact properties. These properties tend to be dictated by the "weakest link in the chain" which in coatings tends to be the particle or grain boundaries and coating-substrate interface. Coatings are limited to the load they can carry, and thus require a substrate for support, even then, coatings are poor when point loaded.

In case for Thermal coatings tensile stresses extremely adversely effect properties. Effective bond strength is reduced and can be destroyed by increasing levels of internal stress. This in turn effects Thermal coating thickness limits. For round surfaces coatings on external diameters can be built up to greater thickness than that on internal diameters.

SIMAT™ minimizes the thermal influence by avoiding a transformation from molten to solid phase of deposited materials. That is one of the explanation to SIMAT™ capabilities to produce thick coatings and built-up three-dimensional structures.

3.3 General Properties Comparison

This comparison generally shows coating properties in a bad light, and does not take into consideration that coatings are usually supported by a substrate. Coatings are generally only used to give surface properties such as wear resistance and not to add strength.

Properties of coatings should be considered in their own right and not the properties of the original material prior to spraying as they can be very different physically and chemically.

PROPERTY	THERMAL POWDER COATING	SIMAT™
Strength	low	low
Ductility	very low	low
Impact	low resistance	good resistance
Porosity	high	low
Hardness	high	low
Wear resistance	high	low
Corrosion	low resistance	high resistance
Machining	poor	good

Table 3.1 Comparison of Thermal Powder coatings to their SIMAT™ equivalents

Chapter 4

SIMAT™ Research Objectives and Experimental Procedure

4.1 Experimental Procedure

Formation of SIMAT™ coating layer only depends on powder mix characteristics and impact conditions during the deposition process. To optimize the process parameters, spray conditions have to be tuned for particular powders. A direct optimization procedure for several powders by varying cold spray conditions is time consuming and costly.

Therefore, alternative test method have been developed which is less expensive and operates with similar load mechanisms on powder particles. High strain rate deformation can be easily studied by a powder compaction method. In this method, the powder mix is loaded in the experimental die with sloping punches and deformed under high stress rates. The method is called a "Shear Compaction" and its goal is to simulate bonding conditions of powder particles similar to those obtained in cold spraying. Considering the fact that the metal powder spray stream is not constrained in horizontal direction we have to bring into account a tangential component of the coating compacting stress. This tangential component is simulated by the certain angle of the die punches. By a special die design with sloping punches, load delivered during powder compaction can cover a wide range of spray parameters in one single experiment. Therefore, the method appears feasible to determine the spray process characteristics for successful bonding of particles with less efforts and less costly than by performing a parameter optimization in cold spraying. To evaluate the capability of the method, microstructural features of particle-particle interfaces were investigated and compared to those of cold sprayed coating. Therefore, experimental strategy provides two directions of tests: direct deposition tests and modeling shear compaction tests. The results of these tests, specifically density and mechanical properties of coated and compacted layers, were compared (Figure 4.1).

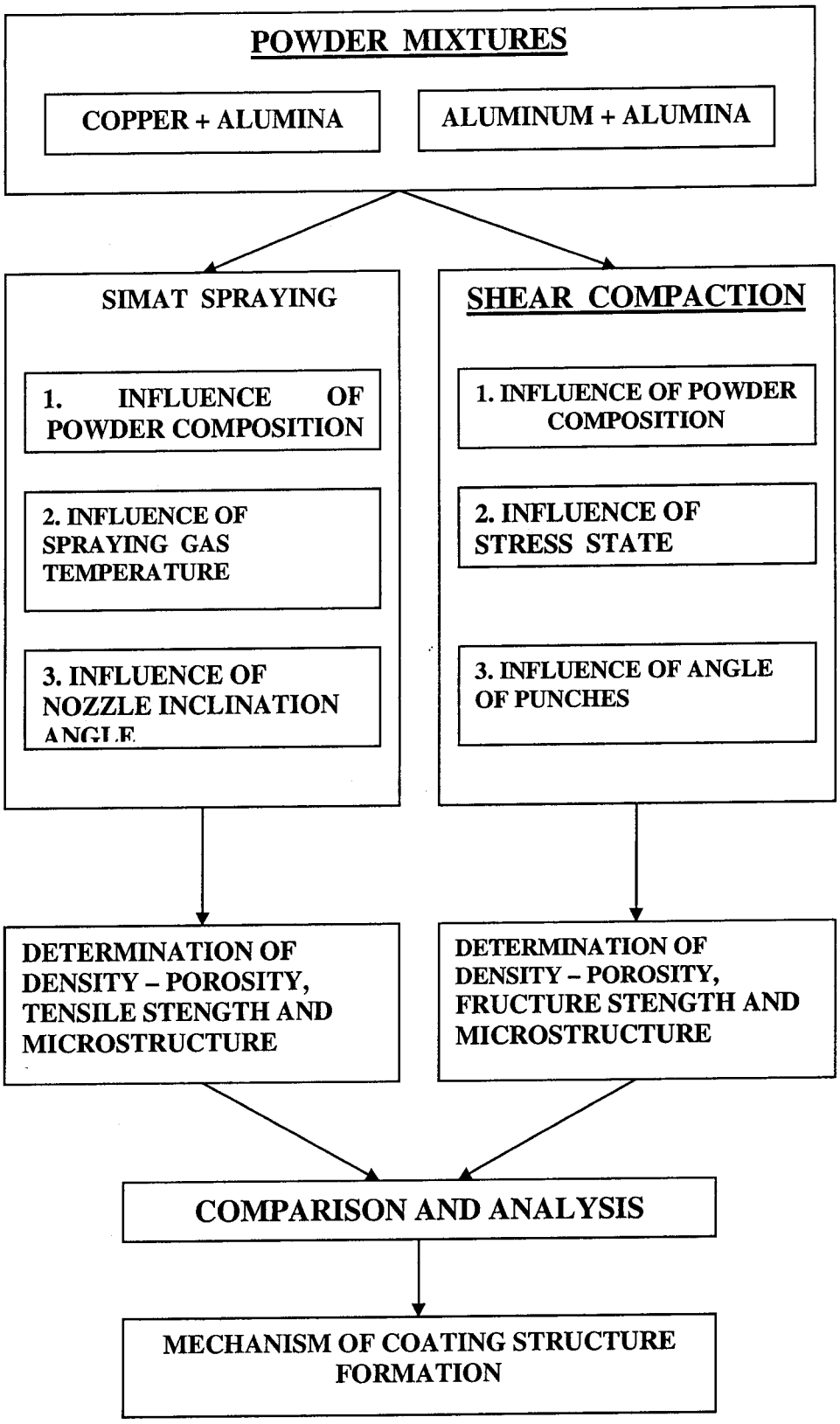

Figure 4.1 Schematic Diagram of Cold Spraying and Shear Compaction Modeling Experimental Procedure

4.2 Determination of Variables and Deliverables

In accordance with Experimental Procedure Variables and Deliverables are shown on the diagram (Figure 4.2) :

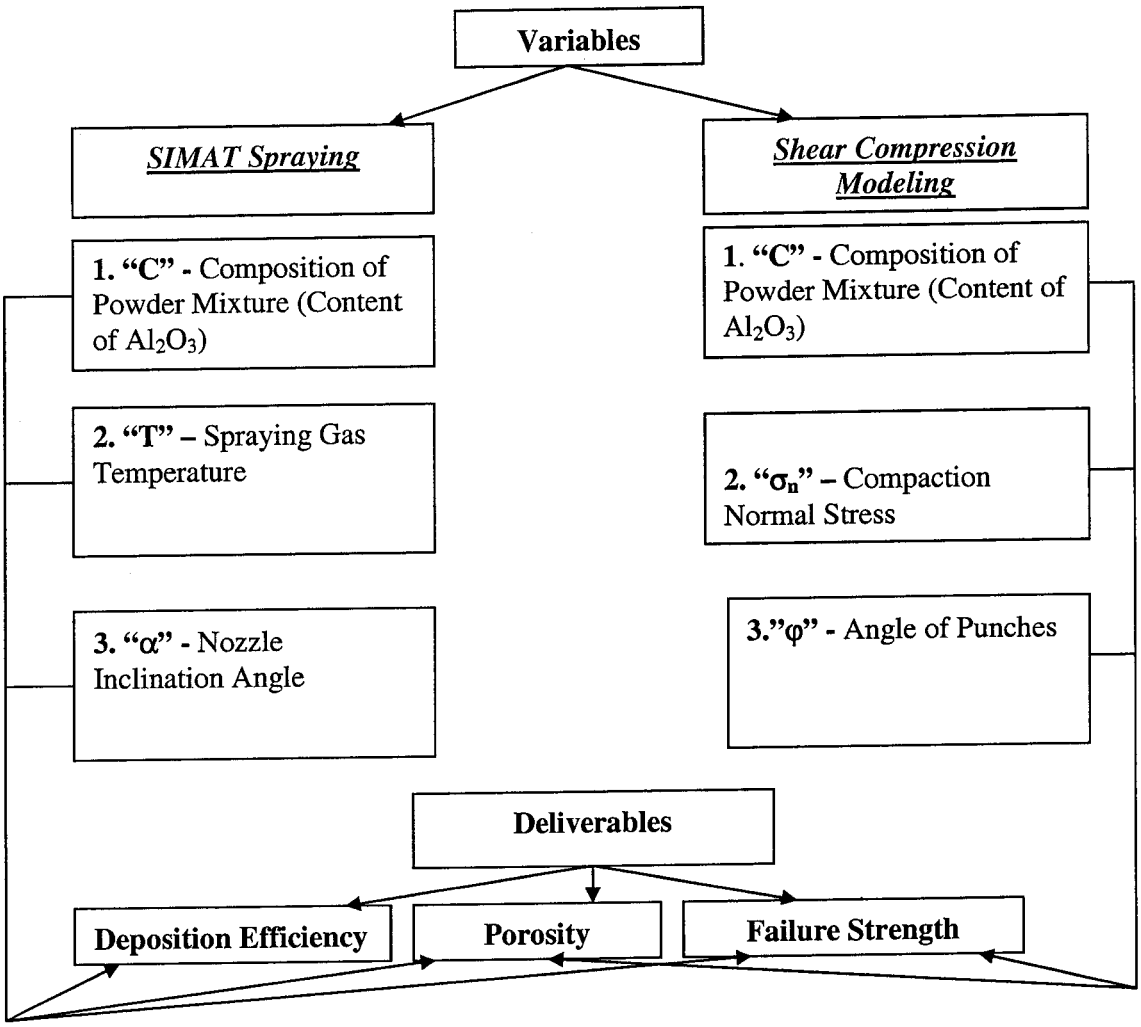

Figure 4.2 Schematic Diagram of Experimental Variables and Deliverables

4.3 Experimental Materials

Materials for study are chosen on the base of previous research results and include Copper powder d=40-50mkm, Aluminum powder d=30-50mkm and Alumna powder

d=10mkm. Compositions of the studied powder mixtures are represented in the next chart (Table 4.1).

COPPER 100%	ALUMINIUM 100%
COPPER + 15% ALUMINA	ALUMINIUM + 15% ALUMINA
COPPER + 25% ALUMINA	ALUMINIUM + 25% ALUMINA
COPPER + 45% ALUMINA	ALUMINIUM + 45% ALUMINA

Table 4.1 Experimental powder mixtures

4.4 Experimental SIMAT Apparatus Set-up

The deposition of samples on steel substrates was performed with installation which is shown on Figure 4.3. The main units of spraying device are gas heater, powder feeder and Laval type nozzle. The last one is inclined with small angles α as shown on Figure 4.3-a. The measured and controlled parameters were:

1. Temperature of gas which was fed under constant pressure of 5.5 Bar, which corresponds to the standard spray air velocity ~ 550 – 600 m/sec
2. Duration of processing was 5 sec
3. Weight of powder which was fed into nozzle
4. Spraying distance **L** was constant (20 mm)

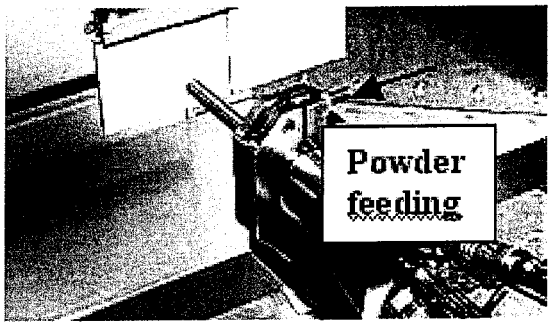

a

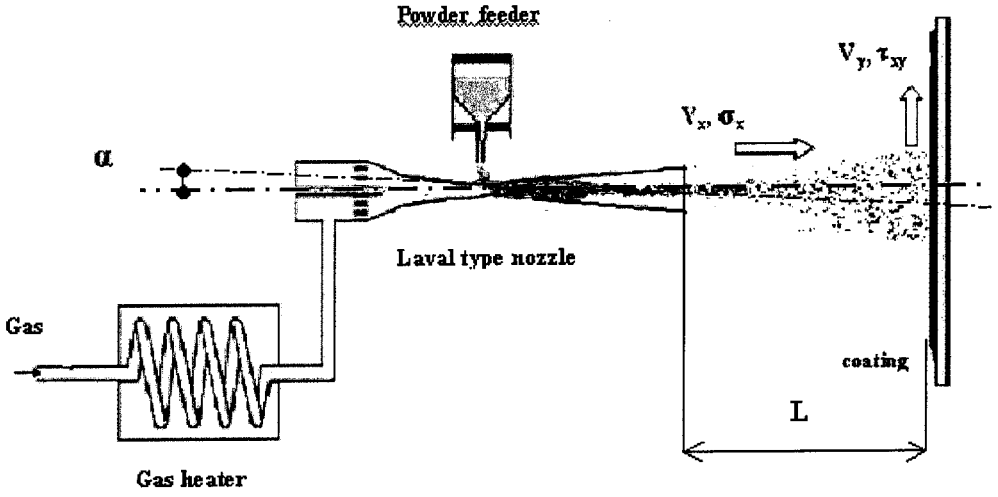

b

Figure 4.3 General view (a) and principal scheme (b) of experimental spraying set-up

4.5 Experimental Shear Compaction Tackle Set-up

The Gas Dynamic Spray Technology allows to produce coatings with a relatively small thickness up to 2-3mm. We received samples with the same thickness from Copper-Alumna powder mixtures by shear compaction technique.

Modeling Shear Compaction tests were performed on INSTRON testing machine with special compaction tool set (Figure 4.3) with different angles and under different loads with various compaction velocities. The pictures below represent the experimental dies and punches and their installation in the press equipment.

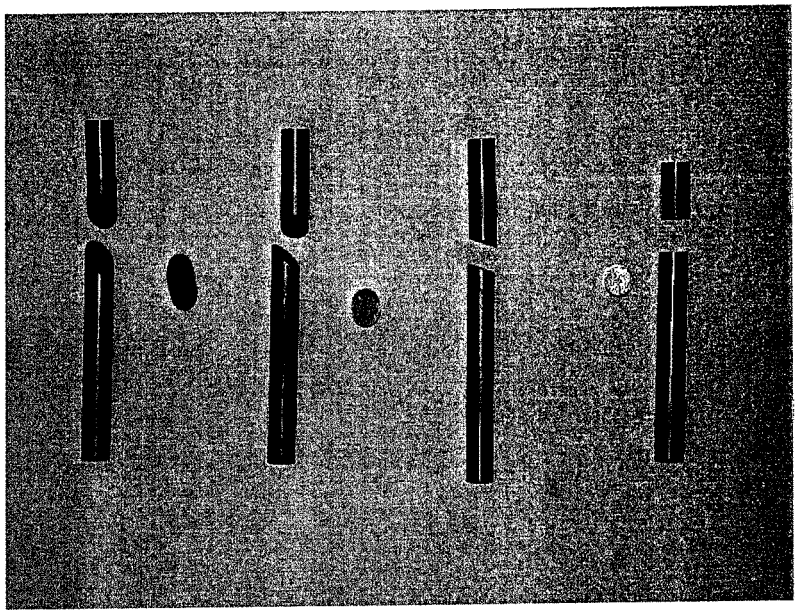

a

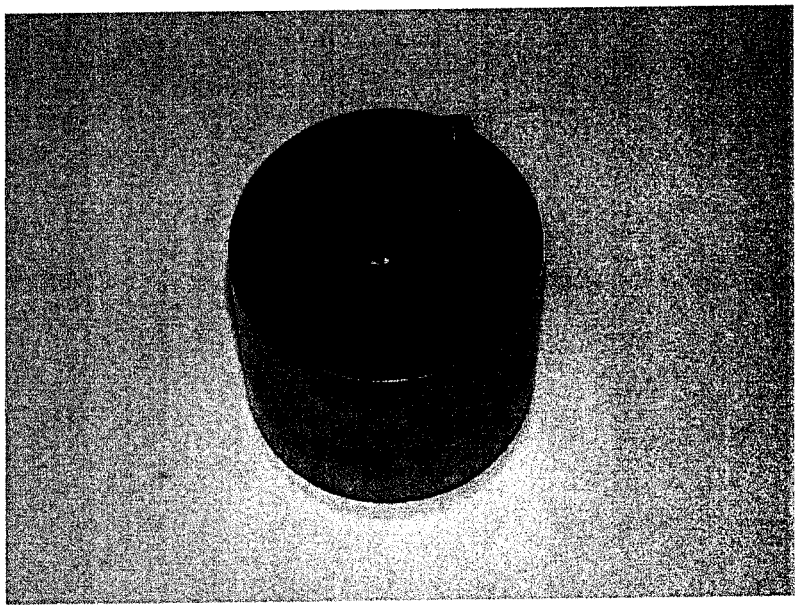

b

Figure 4.4 Shear compaction tool : a - punches and samples
b - matrix with punches

Figure 4.5 Equipment installation on INSTRON 5500 HVL test machine

4.6 Determination of tensile strength of samples for coatings

Tensile tests were performed on INSTRON test machine (Figure 4.6) measuring the force required to break a specimen and the extent to which the specimen stretches or elongates to that breaking point. Tensile tests produce a stress-strain diagram, which we used to determine the material tensile modulus.

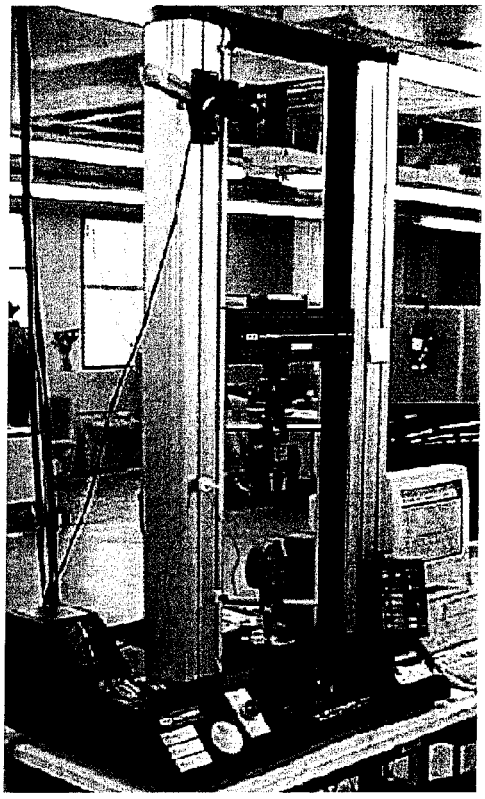

Figure 4.6 INSTRON test machine of 50KN capacity

ASTM D882 defines strips cut from thin sheet or film. For standard ASTM D882 - Thin Sheet- the test speed is typically 5 mm/min for measuring strength and 1mm/min for measuring elongation modulus. An example of test data is shown on Figure 4.7. This type of examination permits to obtain data of percent elongation at break of coating. The data of ultimate tensile strength was received from direct coating sheet tests.

In order to directly determine the tensile strength of coating formed on sheet samples two series of experiments were carried out. The first test is the tensile tests of coatings without substrate. The special samples were prepared by grinding. The second one is the tensile tests of sheet samples with coatings with the same thickness.

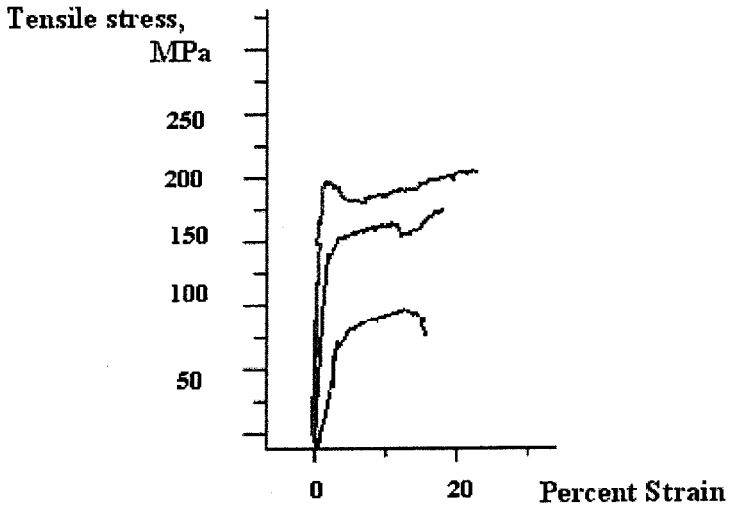

Figure 4.7 INSTRON Stress – Strain diagram example:

1- pure mild steel sample

2-mild steel sheet with deposited copper+25%Al_2O_3 layer

3-single coating of 2 mm thick

Using INSTRON test diagrams the following parameters were derived :

1. Tensile Strength (at yield and break points)
2. Tensile Modulus
3. Strain
4. Elongation and percent of elongation at yield
5. Elongation and percent of elongation at break.

4.7 Determination of Strength of Compacted Samples

The task of estimation of thin layers strength by conventional compression method is not so simple because of significant contacts effect. Firstly, the distribution of contact stresses is indefinite. Secondary, the value of fracture stress is difficult to define

because of a great influence contact normal stresses on fracture properties of the samples of small thickness.

For this reason we offer to define a fracture strength of powder compacted thin disks by diametrical compression as shown on Figure 4.8. The main sense of such a test lies in utilization of a considerable difference between compression and tensile test fixtures for compacted samples of powder materials [1].

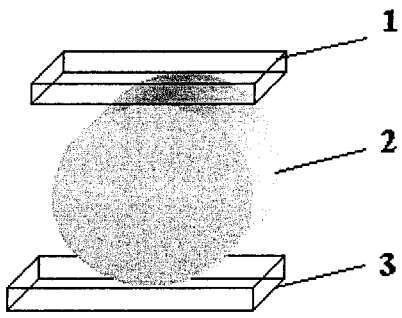

Figure 4.8 Diametrical compression test of a powder disk sample of thickness t :

1-upper plate 2-disk sample 3-down plate

The hardness of loading plate is considered to be low in order to achieve the uniform load distribution . A main indicator of the test scheme validity is a linearity of crack and it's perpendicularity to the loading plates. Compression of an elliptical disks which are made by shear compaction with angle punches (Figure 4.4) did not distort results too much.

Chapter 5

SIMAT™ Process Modeling

5.1 SIMAT™ Parameters Determination

5.1.1 SIMAT™ Spray Process Characteristics

We apply a **rate of powder use** as the main parameter of the **deposition efficiency**.

The deposition efficiency - η- is a ratio of coating weight to weight of powder fed into a nozzle :

$$\eta = \frac{W_{COATING}}{W_{SPRAYED}}$$

The **temperature** range for examination of deposition effectiveness was chosen in the range of 200-600^{0}C on the base of results [13].

The **inclination angle** of a nozzle was varied in the range of 0-15^0.

5.1.2 SIMAT™ Coatings Experimental Characteristics

The qualitative parameters of coatings used for the current research were **density ρ or porosity υ=(1- ρ) and ultimate tensile strength σ_{uts}** of coatings.

5.1.3 SIMAT™ Experimental Characteristics Correlations and Dependences

The spraying examination designated to the determination of the next dependences:

► **the deposition efficiency η** from gas temperature T and powder composition on the base of copper and aluminum - $\eta = \eta(T,C)$,

where C –content of Alumina in powder mixture.

► **the density ρ or porosity $\upsilon=(1-\rho)$** of coatings from **the deposition efficiency η** , gas temperature T and powder composition C : $\rho = \rho(\eta, T, C)$

► **the ultimate tensile strength σ_{uts}** of coatings from **the deposition efficiency η** , gas temperature T and powder composition C : $\sigma_{uts} = \sigma_{uts}(\eta, T, C)$

► **the nozzle inclination** α effect on deposition efficiency η , density ρ, porosity $\upsilon=(1-\rho)$ and ultimate strength $\sigma_{uts} = f(\alpha)$.

Determination of nozzle inclination α effect on deposition efficiency η , density ρ and strength of coatings σ_{uts} was made for two optimal types of powder composition: Cu+25%Alumina at the temperature 600^0C and Al+25%Alumina at the temperature 200^0C .

The experiment data matrix is shown below in Table 5.1.

		Composition					
		Copper-Alumina mixture			Aluminum-Alumina mixture		
		Cu+15% Al_2O_3	Cu+25% Al_2O_3	Cu+45% Al_2O_3	Al+15% Al_2O_3	Al+25% Al_2O_3	Al+45% Al_2O_3
Gas Temperat. T °C	200	η	η	η, ρ, σ_{uts}	η, ρ	η, ρ	η, ρ
	400	η, ρ, σ_{uts}	η, ρ, σ_{uts}	η, ρ, σ_{uts}	-	-	-
	600	η, ρ, σ_{uts}	η, ρ, σ_{uts}	η, ρ, σ_{uts}	-	-	-
Nozzle inclination α^0(T=600 °C)	1	-	η, ρ, σ_{uts}	-	-	η, ρ, σ_{uts}	-
	2	-	η, ρ, σ_{uts}	-	-	η, ρ, σ_{uts}	-
	5	-	η, ρ, σ_{uts}	-	-	η, ρ, σ_{uts}	-

Table 5.1 Matrix of Spraying Parameters Determination

5.2 SIMAT™ Process Modeling Using Shear Compression Technology

5.2.1 Principles of Physical Modeling

The spraying deposition process is characterized by an impact interaction of powder particles' assembly with a substrate. During a such interaction a large quantity of heat is emerged due to a calorific effect . Moreover the powder particles are being plastically deformed under high normal σ_x and shear τ_{xy} stresses and this particular media is densifying and flowing (Figure 5.1).

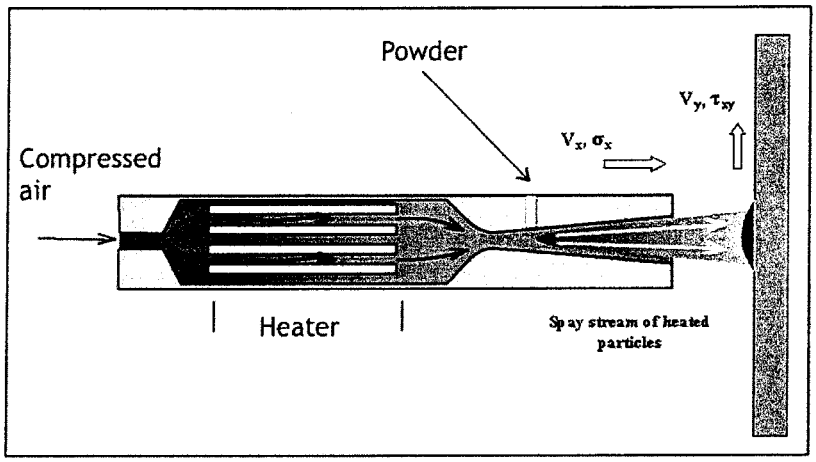

Figure 5.1 Spray stream of powder particles from the nozzle

It is clear that this process can not be analyzed from the viewpoint of individual particle deformation behavior. An assembly of the individual particles which interact one with other flows and changes it's dimensions due to collision of particles with high kinetic energy. The high kinetic energy of the hot powder particles on impact with the substrate result in a build up of a very dense and strong coating

The direct physical modeling of the spraying deposition process and densification of coating is difficult because of lot of factors which influences this process. As the first step of physical modeling we offer to model and analyze the powder densification and consolidation processes from the viewpoint of mechanic of deformable media that treats of the manner in which bodies acts under the loads, or forces, which deform them [2].

The densification of a thin powder layer during it's interaction with a substrate under loads (Figure 5.1) is believed to be modeled by densification of the powder layer of the same composition during axial die compaction. However shear stress components in usual axial die compaction scheme are small and it is difficult to define them because of indefinite value of a radial component of strain velocity $\mathbf{V}_\tau$. For this reason we offer to treat the combined compaction scheme **"compaction +shear"** (**shear compression**) which is performed by an **"angle"** punches (Figure 5.2).

This modeling method virtually enables to determine the stress and strain parameters of particles interaction in real Cold Spraying process. It takes into account the influence of shear strains of the process of the coating structure formation.

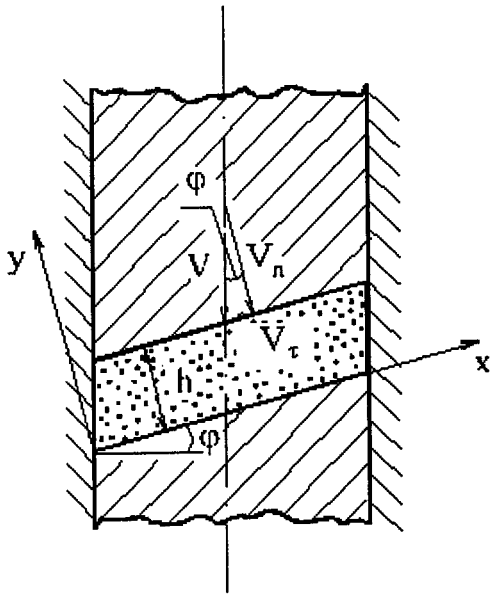

Figure 5.2 Shear compression with "angle" punches

The realization of such a powder compaction technology is performed with a special tool set (Figure 5.3).

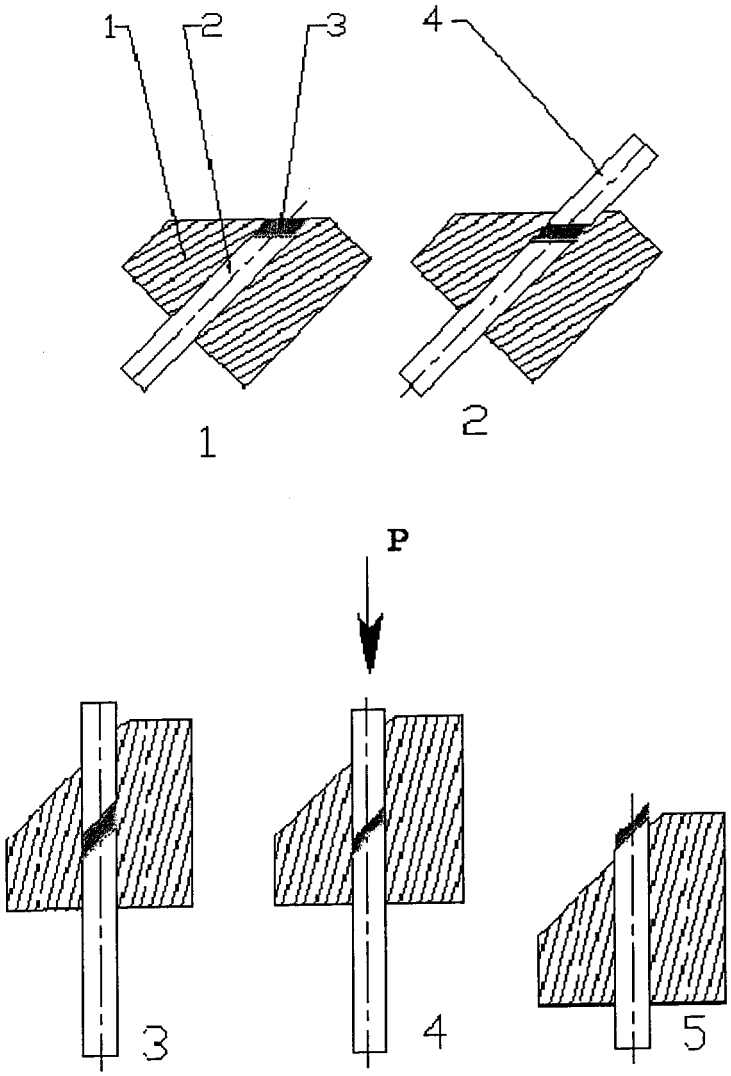

Figure 5.3 Shear compression steps of powder layer

1 - filling die cavity with powder mixture

2 - leading –in upper punch

3 - turning of the tool set in pressing position

4 - compaction of powder layer

5 - ejection of powder compacted disk

The tool set consists of matrix (1), bottom (2) and upper (4) punches. Matrix and bottom punch form a die cavity. The powder mixture (3) is fed into the die cavity by hopper (it is not shown on the Figure 5.3). The tool set is tilted in order to achieve the uniform filling of the matrix cavity. After filling the tool set is turned into the pressing position . The values of normal $\mathbf{V_n}$ and tangential $\mathbf{V_\tau}$ velocity is controlled by the angle φ of punches (Figure 4.2).

5.2.2 The Modeling Task Statement

The aim of physical modeling dynamic spraying process is to define the densification mechanisms of powder mixtures for various composition .
It is known from previous experiments the main technology parameters which influence on density and strength of coating layer are:

1. powder mixture composition
2. powder particles' sizes
3. temperature and velocity of powder stream

The shear compression technology enables to simulate directly powder mixture composition and powder particles' sizes . The temperature of powder stream in our case defines the plasticity and yield strength of powder mixture from one side and bonding of powder particles from second side. As a first step we intend to perform shear compaction experiment at the ambient temperature. So the bonding processes are not simulated completely in this case. Nevertheless the offered method enable to take into account effect of yield strength (σ_s) of powder material by the using of parameter "**dimensionless stress**" that is the ratio σ / σ_s.

Additionally shear compression experiment enables to model the densification process at the different ratios of normal $\mathbf{V_n}$ and shear $\mathbf{V_\tau}$ velocities which are simulated by angle φ of punches .

Therefore the main goal of the modeling is to define dependences of density and fracture strength of deposited powder mixtures from normal stresses, angle of punches and composition of powder mixtures.

5.2.3 Stress Estimation of Particle Media Impact During Spraying

The modeling experiments are needed to be performed in the conditions that are the same as for cold spraying process. For this reason the rough estimation of stress-state parameters for both cold spraying and shear compaction were made.

The cold spraying process is characterized by a particles ensemble impact with substrate.

We assumed that powder ensemble which is fed on substrate and impact with surface may be characterized by cylinder representative element.

Representative element sizes of powder media: $\mathbf{H = d}$ particle $\cdot \mathbf{n}$, where

d particle - means diameter of particle

n - number of particle layers coated immediately

D - diameter of powder stream spot.

Volume of the representative element:

$$v = \mathbf{d}_{\text{particle}} \cdot \mathbf{n} \cdot \pi \cdot \mathbf{D}^2/4 = 1.8 \text{ mm}^3 \quad (D \cong 3 \text{ mm})$$

The force realized by impact of this volume: $\mathbf{F=m \cdot a}$, where

m - mass of representative volume

$\mathbf{m} = \rho_{\text{apparent}} \cdot v$, where ρ_{apparent} is apparent density of powder in powder stream.

An acceleration of this volume is calculated taking into account the approximate time of impact ~5μsec.

Temperature, T	Particle velocity, V(estimated)	Impact force F=m·a	Normal stress σ_n	Yield strength, σ_s (Cu)	Dimensionless normal stress, σ_n/σ_s
^{0}C	m/s	N	MPa	MPa	
0	150	4320	480	40	12
200	200	5760	640	20	32
400	400	11520	1280	10	128
600	600	17280	1920	4	480

Table 5.2 Results of stress parameters estimation for Cold Spraying

The results of estimation are shown in Table 5.2 .

The comparison of calculated relations σ_n/σ_s with those for shear compaction modeling shows that we have two ways to receive the same values of such similarity parameter:

1. Interpolation of compaction experimental results to values of σ_n/σ_s in the wide range of 20-400
2. Examination of compaction process at the high temperature in order to sharply decrease the yield stress of powder particles.

As the first step we apply the first way of experimental dependences approximation.

5.2.4 Estimation of Strain Sate Conditions for Cold Spraying

Shear velocity of the representative element of powder volume of 1.8 mm^3 (D=3mm) (Fig.5.2)

$$V_x=V_{spraying}\cdot sin\alpha \ ;$$

The shear displacement is calculated as

$$\Delta = V_x \cdot dt \ ,$$

where dt is the time of impact (~5μsec) , shear strain is :

$$\gamma_{spraying} = \frac{\Delta}{H_i} = \frac{V_{spraying} \cdot \sin\alpha \cdot dt}{H_i}$$

The results of calculations are shown in Table 5.3.

5.2.5 Estimation of Strain State Conditions for Shear Compaction Modeling

The powder compaction scheme is shown on Figure 5.2. The stress-strain state for thin layer of powder media is assumed to be uniform. So during upsetting of powder layer with plates we have

$$V_n = V \cdot \cos\varphi, V_\tau = \sin\varphi \qquad \text{at} \quad y=h$$

The velocities distribution is:

$$V_x = -\frac{V_\tau}{h} \cdot y = -V \cdot \sin\varphi \cdot \frac{y}{h}$$

$$V_y = -\frac{V_n}{h} \cdot y = -V \cos\varphi \cdot \frac{y}{h}$$

The strain rates are determined as:

$$\xi_x = \frac{dV_x}{dx} = 0, \xi_y = \frac{dV_y}{dy} = -\frac{V \cdot \cos\varphi}{h}; \xi_z = 0;$$

$$\eta_{xy} = \frac{dV_x}{dy} + \frac{dV_y}{dx} = -(V \cdot \sin\varphi)/h$$

Shear strain in the case of shear compaction is calculated as

$$\gamma_{\text{compaction}} = \eta_{xy} \cdot t ,$$

where t is a time of compaction process with velocity $V_{\text{compaction}}$

The compaction parameters t =10 sec, H = 3 mm, $\varphi = 20^{\circ}, 40^{0}, 50^{0}$ were applied.

Thus the similar cold spraying and shear compaction strain conditions are:

$$\gamma_{\text{spraying}} = \gamma_{\text{compaction}} .$$

So, after inserting above relations we can calculate shear compaction velocity which provides the similarity conditions with Cold Spraying :

$$V_{comp} = \frac{\gamma_{spraying} \cdot H}{\sin\varphi \cdot t}$$

Results of calculations are shown in Table 5.3:

Nozzle Inclination angle	Spraying Impact time ~5μsec				Punch Angle	Shear Compaction			
α	V_{spr}	V_x	Δ	γ	φ	V_{comp}	H	t	γ
^{0}	m/s	m/s	μm		^{0}	mm/s	mm	sec	
0	600	-	-	-	0	5	3	10	-
1	600	10.47	52.35	0.26	10	0.22	3	10	0.26
2	600	20.95	104.7	0.52	40	0.24	3	10	0.52
3	600	31.2	155	0.775	50	1.17	3	10	0.775

Table 5.3 Calculation of Spraying and Compaction parameters on the base of shear strain parameter similarity.

5.3 Modeling Experimental Procedure

The experimental strategy of study provides two directions of tests: direct deposition tests and modeling shear compaction tests. Modeling shear compaction tests was performed on testing machine with special compaction tool set (Figure 5.3) with various compaction velocities (Table 5.2.). Additionally SEM (Scanning Electron Microscopy) analysis were made.

Materials for study are chosen on the base of previous research results and include Copper powder d=40-50mkm and Alumna powder d=10mkm. Compositions of powder mixtures to be studied are :

- Copper
- Copper+15% Alumna
- Copper+25% Alumna
- Copper+45% Alumna.

The rupture strength was determined by diametrical compression of powder disks. The background of application and description of diametrical compression tests are shown below.

5.4 Determination of Strength of Samples

The Gas Dynamic Spray Technology allows to produce coatings with a relatively small thickness up to 2-3mm. We received samples with the same thickness from Copper-Alumna powder mixture by compaction technique . The task of estimation of thin layers' strength by conventional compression method is not so simple because of significant contacts effect. Firstly, the distribution of contact stresses is indefinite . Secondary, the value of fracture stress is difficult to define because of a great influence contact normal stresses on fracture properties of the samples of small thickness.

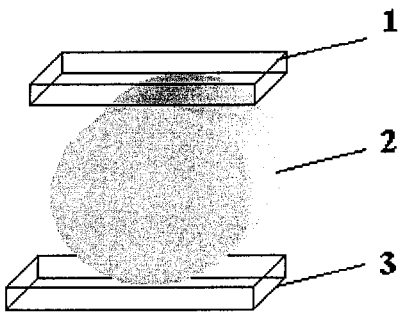

Figure 5.4 Diametrical compression test of a powder disk sample

1 - upper plate, 2 - disk sample, 3- lower plate.

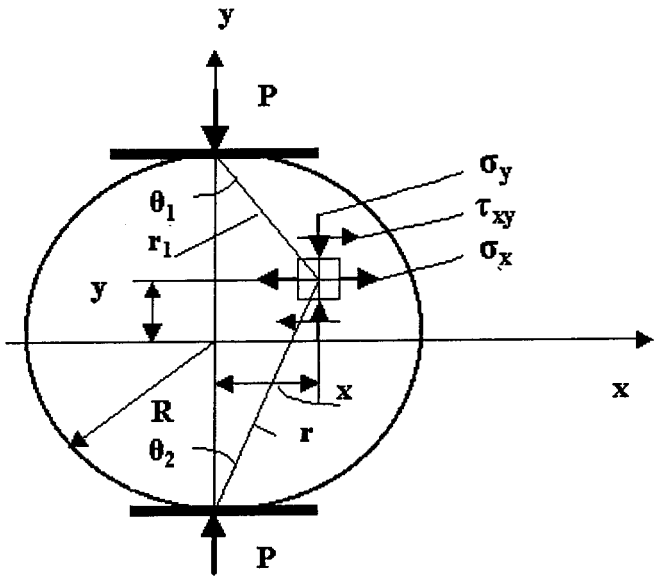

Figure 5.5 The scheme of forces acting during diametrical compression test of disk

For this reason we offer to define a fracture strength of powder compacted thin disks by diametrical compression as shown on Figure 5.4. The main sense of such a test lies in utilization of a considerable difference of compression and tension strength of compacted powder materials [1]. During diametrical compression of cylinder sample by plates (Figure 4.4) the maximum normal tension stresses σ_x arise in the direction which is the normal to the vector of load (P) applying (Figure 4.5). These tension stresses generate a fracture in the diametrical plane that passes trough points of contact with loading plates.

According Frocht [1] stresses in any point of disk are determined by equation

$$\sigma_r = \frac{2P}{\pi t} \cdot \frac{\cos\theta}{r} ,$$

where: r - is absolute value of radius-vector turned from point of load applying to the element (x,y);

t – the thickness of disk;

θ - the angle between vectors P and r.

Frocht [1] also showed (denotations are on Figure 5.5) :

$$\sigma_x = \frac{2P}{\pi t d},$$

$$\sigma_y = \frac{2P}{\pi t}\left[\frac{2}{d-2y} + \frac{2}{d+2y} - \frac{1}{R}\right].$$

The width a of contact area between the sample and loading plate is determined with relation

$$a = 1.6\sqrt{\frac{P \cdot d\,(1-\mu_S)^2}{t \cdot E_{Plate}}},$$

taking into account that Young's modulus of the loading plate E_{Plate} differs significantly from modulus of elasticity of the disk sample E_{Sample} : $E_{Plate} \Uparrow\Uparrow\Uparrow E_{Sample}$.

Here μ_S is Poisson ratio of the disk sample.

The hardness of loading plate is considered to be low in order to achieve the uniform load distribution . A main indicator of the test scheme validity is a linearity of crack and it's perpendicularity to the loading plates. Compression of an elliptical disks which are made by shear compaction with angle punches (Figure 4.2) did not distort results too much.

Chapter 6

Results and Discussion

6.1 Coating Experiments

The experimental results of SIMAT process study are needed to be analyzed from the viewpoint of :

1. Correspondence of the coating parameters to the spray gas temperature accordingly (see Research Objectives) and it's connection with particles' plastic deformation
2. Deformation nature and influence of Alumina content on the deposition efficiency η and density of the deposited layers on the base of Aluminum and Copper
3. Influence of the nozzle inclination angle on the deposition efficiency, density and mechanical properties of coating.

6.1.1 Influence of Spray Temperature on the Deposition Parameters and its correlation with Critical Velocity Concept

The correspondence of Critical Velocity Concept – CVC - to experimental results of Deposition Efficiency appears to be estimated form the comparison of data shown in Table 6.1, Figures 6.1 and 6.2.

Temperat.. ^{0}C	Alumina content, %			
	0	15	25	45
20	11.8	15	15.2	19.4
200	9.5	11.4	10.6	15.5
400	7.3	9	7.8	11.9
600	4	5.2	3	9.2

Table 6.1 Deposition effectiveness(%) of Copper coating

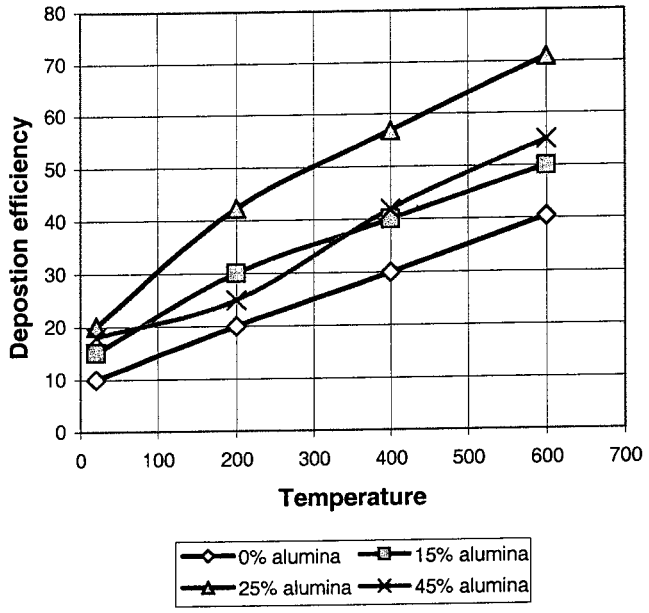

Figure 6. 1 Deposition efficiency -Gas temperature dependence for Cu-Alumna mixtures

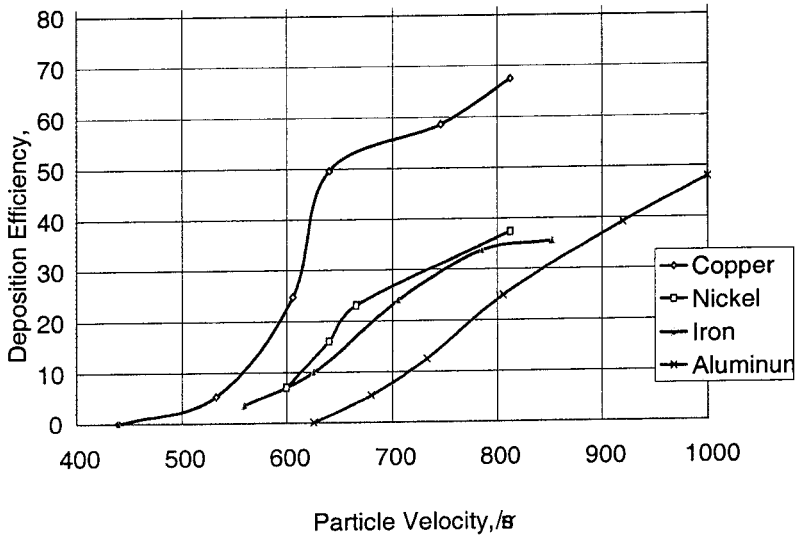

Figure 6.2 Deposition Efficiency –Particle Velocity dependence accordingly to Gilmore [13].

Experimental results of Gilmore (the data from [13]) reveal that high values of η in the range of 50-60% are observed for particle velocity of 600-700 m/s. We received $\eta - T$ dependences for Copper - Alumna mixtures coating (Figure 6.1). It may be concluded from these data:

1. The increase of gas temperature is analogous to increase of particle velocity
2. Deposition Efficiency for copper was achieved in the range of 40%. These values comply with particle velocity near to critical (see Figure 6.2).

It may be clear from Figure 6.2 that Cold Spraying process is realized mostly effectively for metals with high ductility and low yield strength, especially for Copper. The low deposition efficiency for Aluminum is explained usually by stable oxide films on powder particles that prevent bonding [2].

An increase of particles' velocity leads to increase of their kinetic energy, particles' deformation and heat generation during a collision with substrate [9] . Due to these factors the deposition efficiency rises. It is known [5] that the temperature rise increases the stream velocity. But from other side the temperature increase diminishes the yield strength of ductile metal . So the particles' deformation processes during particles impact become easier. For this reason the temperature effect on deposition efficiency which is seen on dependences $\eta - T$ for Copper - Alumna mixtures (Figure 6.10) is analogous to velocity influence.

6.1.2 Influence of Alumna Content

An incorporation of hard Alumna - Al_2O_3 particles into ductile metal powder leads to essential enhancement of interaction between material being deposited and substrate. For this reason the increase of Al_2O_3 content results in increase of deposition efficiency (Figures 6.1 ,6.3) . This effect reveals additional enhancement

of the particles deformation processes during of powder media collision with a substrate surface. The deformation of hard particles of Al_2O_3 does not occur and these particles play a role of "micro-anvils". The intensive plastic flow of ductile metal particles is realized between such "micro-anvils". Additionally ,as assumed by Maev [4], the hard Alumna particles may run through an ensembles of metal particles that leads to ones plastic flow. These processes result in particles bonding because the surface films on the particles are destroyed during particles deformation and diffusion processes are significantly intensified .

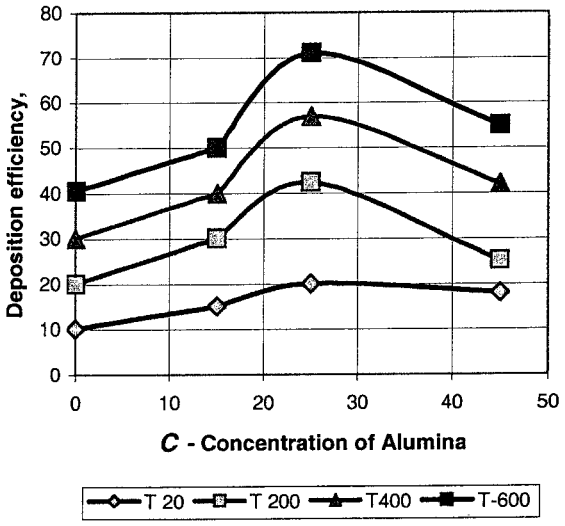

Figure 6.3 Deposition efficiency(%) - Alumna content(%) relationship for the Copper - Alumna mixtures

However, dependence $\eta = \eta(C)$ (Figure 6.3) has a maximum at the Alumna content of 25%. The increase of Alumna content to 45% results in decrease of deposition efficiency. These data reveal qualitative change of coating structure formation mechanisms. The effect of hard Al_2O_3 particles on the deformation of metal powder phase is decreased . As a result the deposition efficiency is diminished. One can assume that the main reason of this effect is mutual collisions and stick of hard Al_2O_3 particles at the high content of Al_2O_3. As a result a network of these connected hard particles is created that prevents the plastic flow of ductile metal particles because of small distance between hard particles.

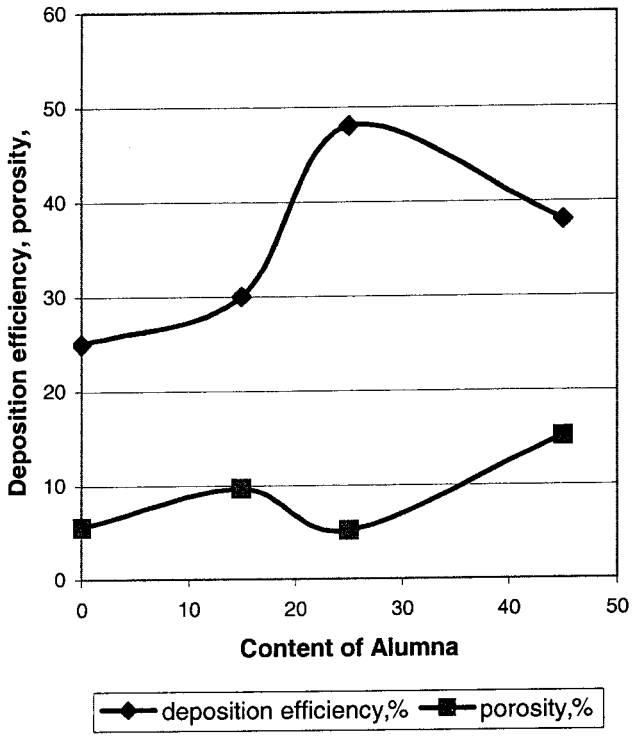

Figure 6.4 Deposition efficiency and Porosity versus Alumna content for Al-Alumna mixtures

The creation of such hard particles network is described and explained by Percolation theory [1,2,3]. The interparticle boundaries are, in some way, pinned by surface oxides or other debris during the deposition process. The moment when particles organize such a network is called as a critical percolation point.[2,3]. At this moment the hard particles cannot affect on metal powder particles . Thus the deformation of metal particles is diminished. This process results in fall of the deposition efficiency on the plot $\eta = \eta(C)$ (Figure 6.3). The same effect occurs at SIMAT spraying of Al + Al_2O_3 powder mixtures (Figure 6.4).

Intensifying of powder media deformation by incorporation of hard Al_2O_3 particles into powder mixture leads to a change of densification . The dependences of coating porosity and Alumna content for Copper powder mixtures are shown in Table 5.2 and Figures 6.5, 6.6.

Temperat.. ^0C	Alumna content, %			
	0	15	25	45
20	11.8	15	15.2	19.4
200	9.5	11.4	10.6	15.5
400	7.3	9	7.8	11.9
600	4	5.2	3	9.2

Table 6.2 Porosity (%) of Copper - Alumna coatings

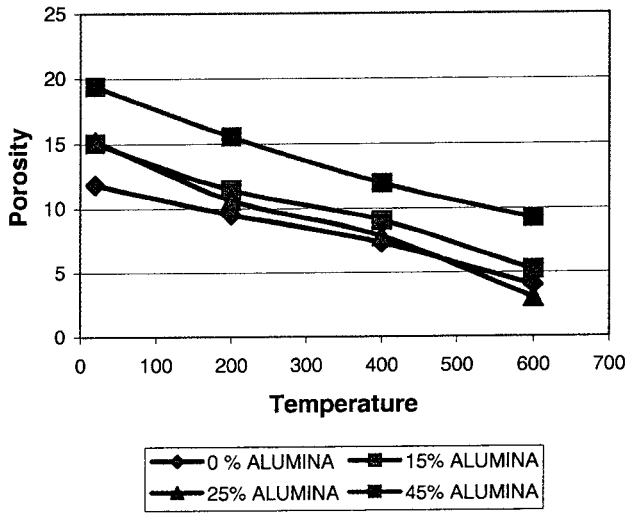

Figure 6.5 Porosity (%) – Temperature (^oC) dependence for Copper - Alumna mixtures

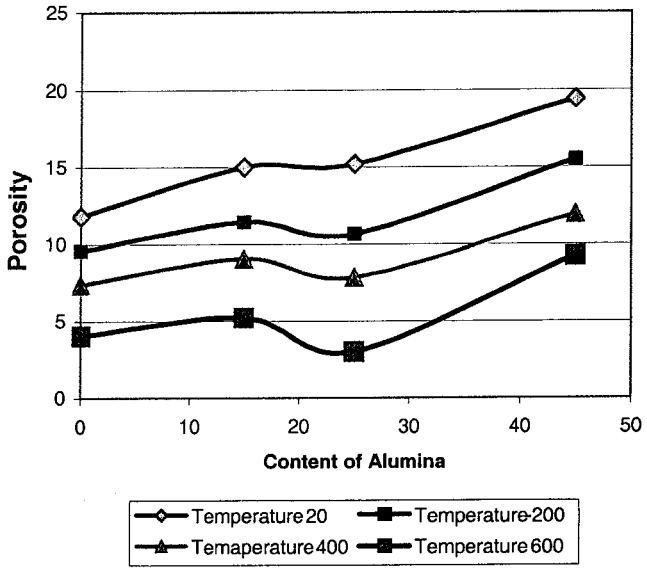

Figure 6.6 Porosity (%) – Alumna content(%) Dependence for Cu-Alumna mixtures

Analysis of the data shown on Figure 6.5 reveals that increase of gas temperature leads to increase of coating density while increase of Alumna content results in decrease of coating density (increase of porosity on Figure 6.6) in spite of increase of the deposition efficiency (Figure 6.3). However one can note that there is a minimum on the porosity - Alumna content curve (Figure 6.6). So, the intensifying of densification is observed at the 25% content of Al_2O_3 particles in Copper powder. The minimum of porosity is observed more clearly for coating at the gas temperature of 600°C. One can assume that the main reason of the effect is a low yield strength or, in other words, plastic flow resistance of Copper particles. The additional heat generation effects leads to increase of particles temperature from 600°C (gas temperature) to temperatures near to melting point. So, yield strength of Copper at this temperature is about 4MPa (see Table 4.1). For this reason the conditions for development of assumed above mechanism of powder media deformation are believed to be more favorable.

This minimum on the plot (Figure 6.6) is according to maximum of the deposition efficiency on the Figure 6.3. This fact reveals that there is an optimal content of hard

particles concentration which provides intensive plastic flow and bonding of particles during SIMAT coating process. The further increase of hard particles content results in increase of plastic flow resistance that leads to fall of both deposition efficiency and density.

6.1.3. Influence of Nozzle Inclination

The intensive plastic flow of powder media during formation of SIMAT coating occurs due to the influence of external forces or loads which cause normal and shear stresses and strain in the interior of the powder body [4] . The normal stress are controlled by the particle velocity at the moment of impact while the shear stress may be changed by other technology parameters such as sizes of Laval Nozzle, angle of Nozzle inclination and distance between nozzle and the substrate surface (see Figure 4.2 Experimental Procedure). So the task of this experimental series is to determine the influence of nozzle inclination angle on SIMAT process parameters as well as the structure and properties of coatings.

As mentioned above coating experiments were performed on the Copper + 25%Alumna and Aluminum + 25%Alumna powder mixtures. The plot of the deposition efficiency is shown on Figure 6.7. These data reveal that the deposition efficiency η falls with nozzle inclination angle increase and tends to zero from the angle of 25°. However a little maximum occurs in the field of small inclination angles α (Figure 6.8). The deposition efficiency is increased on 3 - 5% as compared to the initial values of η (α =0). The inclination of nozzle results in creation of V_X velocity component (see scheme on Figure 4.2 of Experimental Procedure). A displacement of particles in X - direction leads to large shear deformations of powder media. The shear deformation of powder media intensifies a densification of coated layers (Figure 6.9).

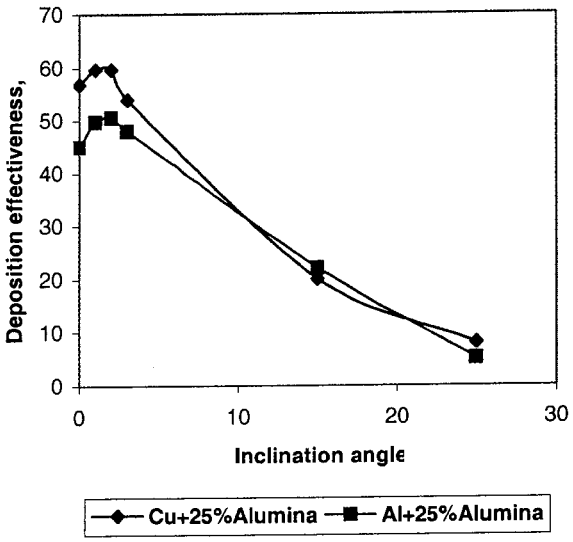

Figure 6.7 Deposition efficiency – nozzle inclination dependence

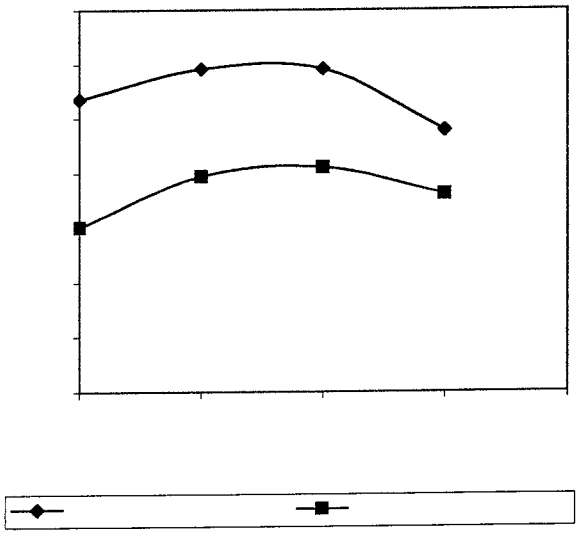

Figure 6.8 Deposition efficiency – nozzle inclination dependence

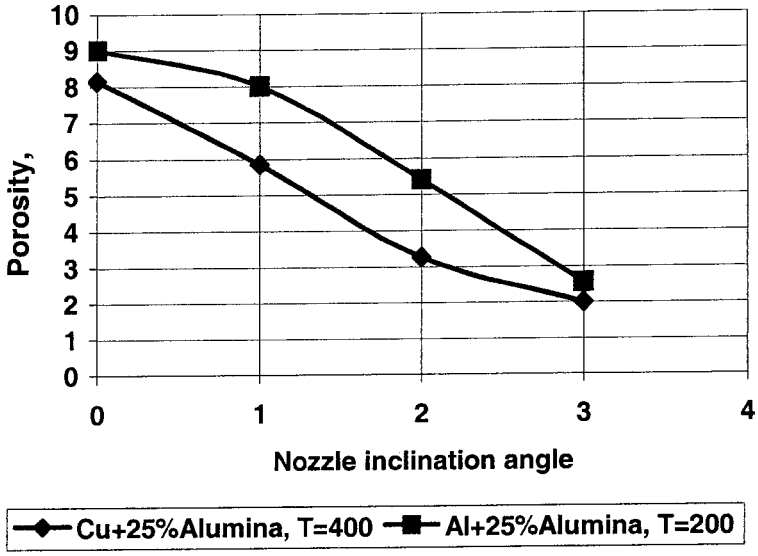

Figure 6.9 Porosity versus nozzle inclination angle for Copper - Alumna and Aluminum – Alumna Mixtures

These data show the strong influence of shear stresses and strains on the densification and ,of course, structure formation for powder mixtures in SIMAT process.

An estimation of stress strain state of powder layer being densified during SIMAT Spraying made in part IV Modeling reveals that a slight increase of inclination angle α sharply raises a particles displacement and shear strain, approximately up to $\gamma =$ 0.77 , see Table 4.2, Modeling.

6.1.4 Mechanical Properties of SIMAT coatings

The results of coating mechanical properties examination (Figure 6.10) show that ultimate tensile strength σ_{uts} of deposited layers depends on α . σ_{uts} raises with increase of α up to 90 - 100 MPa both for Copper and Aluminum powders.

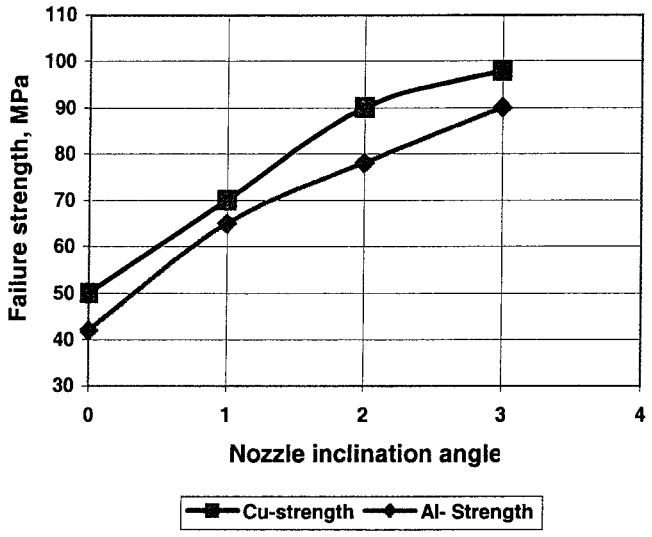

Figure 6.10 Ultimate tensile strength - inclination angle dependence of SIMAT coatings

One should note that the increase of Alumna content in powder mixture raises the ultimate tensile strength as well as the hardness of coatings as shown in Table 5.3.

Inclination Angle, α^o	Shear Strain, γ	Ultimate Tensile Strength (σ_{uts}),MPa		
		Cu	Cu+15%Al_2O_3	Cu+25%Al_2O_3
0	0	50	60	62
1	0.26	71	85	89
2	0.52	89	121	127
3	0.77	98	142	151

Table 6.3 SIMAT coatings ultimate tensile strength (σ_{uts}) examination results

The results of general examination of physical mechanical properties of SIMAT coatings are shown in Table 6.4.

	Al-based coating	Cu-based coatings	Zn-based coatings
Density	**97-98 %**	**97-98 %**	**97-98 %**
Adhesion	**84MPa**	**80MPa**	**88MPa**
Ultimate Tensile Strength	**90MPa**	**94MPa**	**86MPa**
Young's Modulus	**80GPa**	**90GPa**	**84GPa**
Shear Modulus	**30GPa**	**26GPa**	**32GPa**
Poisson's Ratio	**0.29**	**0.32**	**0.34**
Hardness (HV)	**98**	**106**	**94**
Thermal Conductivity	**180W/m**	**360W/m**	**92W/m**

Table 6.4 Physical mechanical properties of SIMAT coatings

The main conclusion from these data is the high effectiveness of SIMAT cold spraying process for ductile metal powders due to intensification of particle media deformation by hard particle additives and variation of process parameters such as temperature, nozzle inclination angle . High density, mechanical properties and thermal conductivity ensure to apply such coatings in a large area of automotive, household machinery and other industries.

6.2 Modeling Experiments

6.2.1 Shear Compression

The tasks modeling compaction of powder media during spraying deposition by shear compression is to determine dependences of density (or porosity) and fracture strength of compacts from compaction pressure, powder composition and shear strains.

The two series of tests were performed:

- compaction of discs of sizes of d = 15mm and height 5mm with shear compaction tool (Figures 5.3), and
- diametrical compression of compacted disks .

The measurement of compacts density was performed by weighting. Fracture strength was determined from the data of diametrical compression with equation (3). The density values of powder mixture constituents are :

- Copper – 8.94 g/cm^3
- Alumna – 4.0 g/cm^3.

For each powder composition the theoretical full density was calculated . Four powder compositions were chosen for experiments:

1. A_1: Copper –100% - full density - 8.94g/cm^3
2. A_2 : Copper 85% + Alumna15% - full density - 8.2g/cm^3
3. A_3 : Copper 75% + Alumna25% - full density - 7.71g/cm^3
4. A_4 : Copper 55% + Alumna45% - full density - 6.72g/cm^3 .

For all experiments the relative density ρ and porosity $v = 1 - \rho$ were calculated as well.

In order to compare all data for different powder mixtures from the viewpoint of it's compatibility it's necessary to take into account yield strength σ_S of each powder mixtures that is dependent of it's composition. On the base of compression tests of sintered samples we approved such values of yield strength for our compositions:

$$\sigma A_1 = 220 \text{ Mpa}$$

$$\sigma A_2 = 265 \text{ Mpa}$$

$$\sigma A_3 = 300 \text{ Mpa}$$

$$\sigma A_4 = 380 \text{ Mpa}.$$

The typical compaction curves are shown in Figure 6.11.

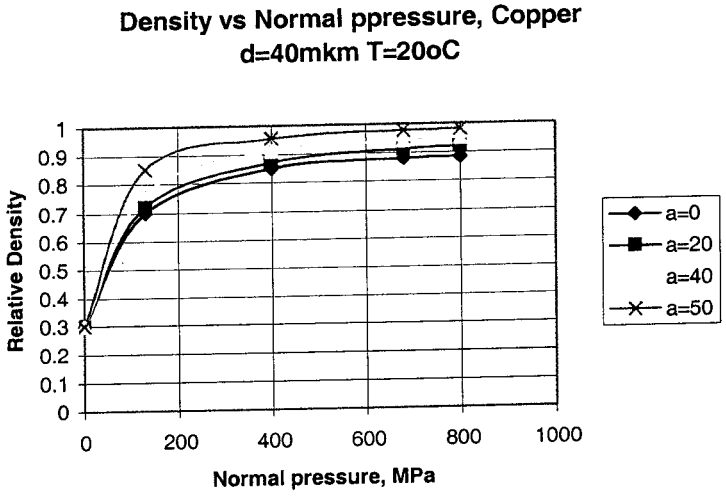

a)

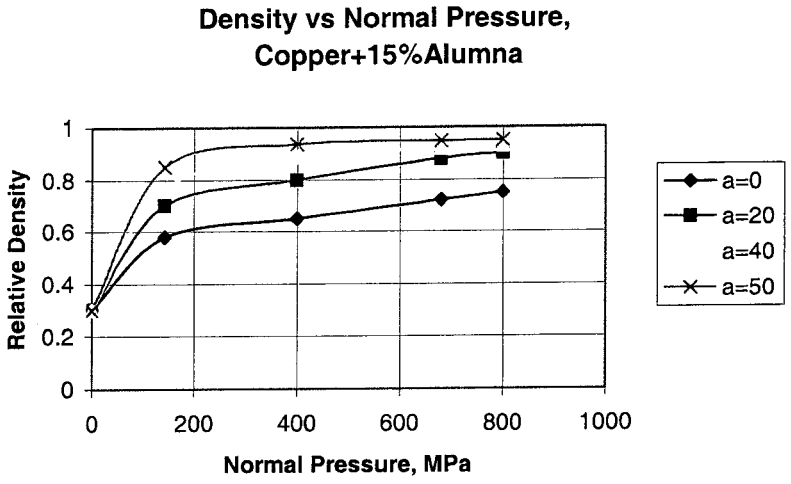

b)

Figure 6.11 Compaction curves for Copper powder (a) and for Copper-15%Alumna mixture (b).

a=0;20;40;50 – corresponds to punches angle φ=0^0; 20^0; 40^0; 50^0.

The compaction curves as a dependences of porosity υ from relative compaction normal stress σ_n / σ_s are shown in Figure 6.12 a,b,c,d.

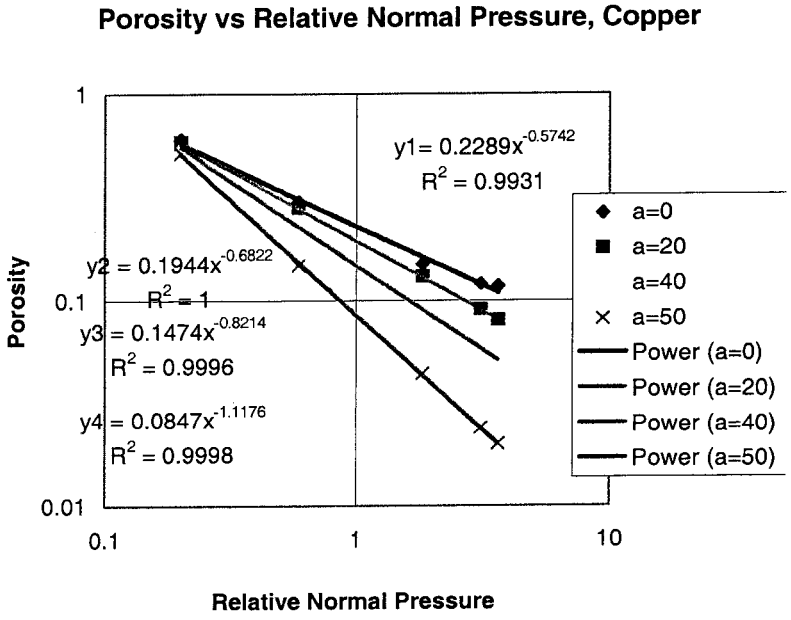

a)

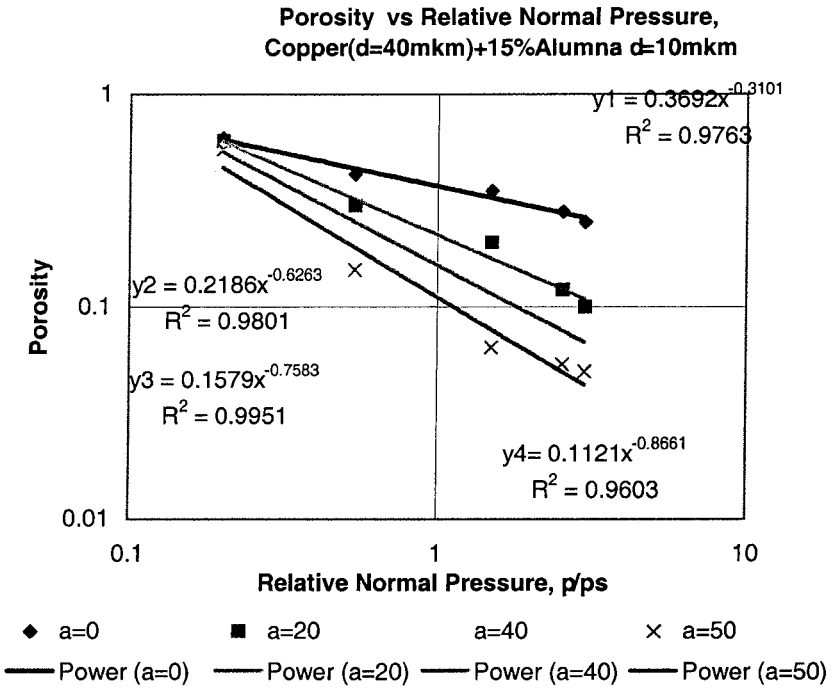
Porosity vs Relative Normal Pressure,
Copper(d=40mkm)+15%Alumna d=10mkm
y1 = 0.3692x^-0.3101
R^2 = 0.9763
y2 = 0.2186x^-0.6263
R^2 = 0.9801
y3 = 0.1579x^-0.7583
R^2 = 0.9951
y4= 0.1121x^-0.8661
R^2 = 0.9603
Porosity
Relative Normal Pressure, p/ps
1
0.1
0.01
0.1
1
10
a=0
a=20
a=40
a=50
Power (a=0)
Power (a=20)
Power (a=40)
Power (a=50)

b)

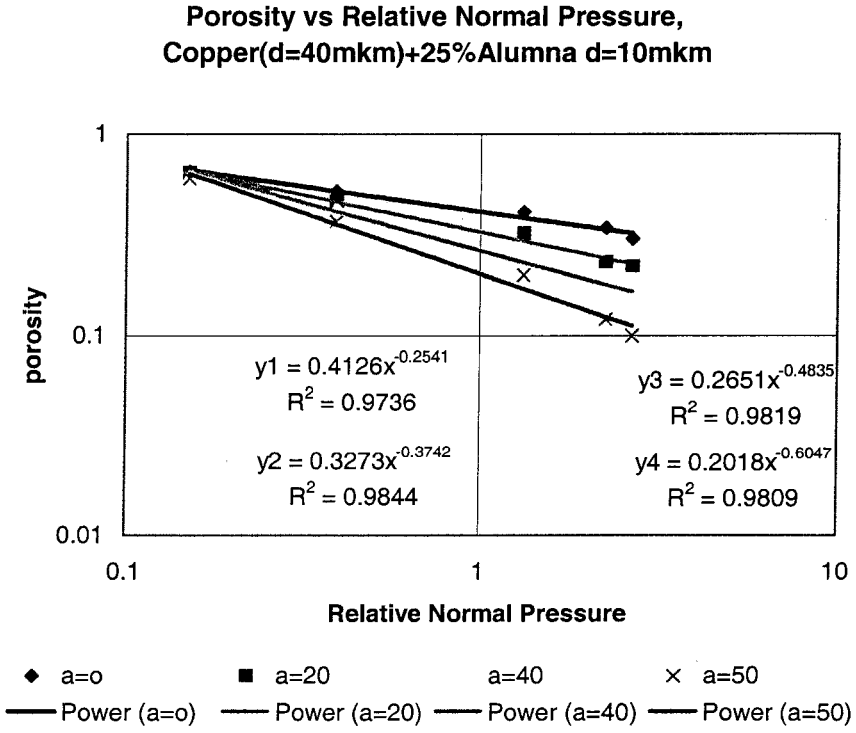
Porosity vs Relative Normal Pressure,
Copper(d=40mkm)+25%Alumna d=10mkm
y1 = 0.4126x^-0.2541
R^2 = 0.9736
y2 = 0.3273x^-0.3742
R^2 = 0.9844
y3 = 0.2651x^-0.4835
R^2 = 0.9819
y4 = 0.2018x^-0.6047
R^2 = 0.9809
porosity
Relative Normal Pressure
1
0.1
0.01
0.1
1
10
a=o
a=20
a=40
a=50
Power (a=o)
Power (a=20)
Power (a=40)
Power (a=50)

c)

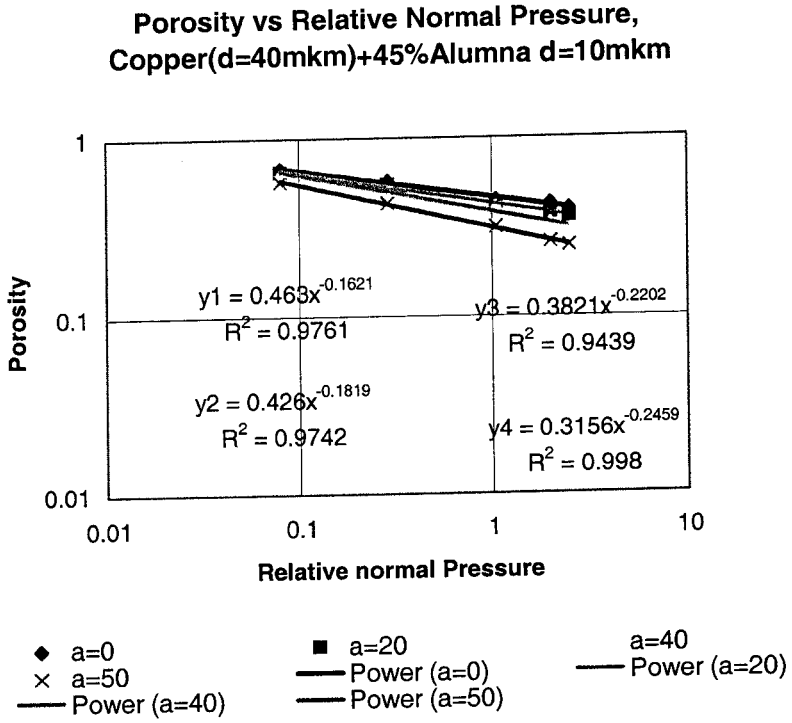

d)

Figure 6.12 Dependences $\upsilon = \upsilon\ (\sigma_n / \sigma_s)$ as a power approximations of experimental data for compaction with different angle punches (in logarithmic scale).

a=0;20;40;50 – corresponds to punches angle φ=0^0; 20^0; 40^0; 50^0.

The experimental results show that increasing of alumna content in powder mixture sharply diminish its compressibility, while the increasing of punch angle enables to achieve higher density with lower compaction stresses . For example,a power approximation equation for simple compaction ($\varphi = 0^0$) of copper powder (A_1) is

$$\upsilon_1 = 0.2289(\sigma_n / \sigma_s)^{-0.572},$$

while for simple compaction ($\varphi = 0^0$) of mixture (A_4) we have an equation:

$$\upsilon_2 = 0.463\,(\sigma_n / \sigma_s)^{-0.1621}.$$

The value of exponent in the case of compaction of A_4 mixture is much lower (by factor 3) as compared to A_1. This parameter defines an angle of slope of approximation line on graph $\upsilon = \upsilon\,(\sigma_n / \sigma_s)$ (see Figure 6.12) . So, in order to achieve the theoretical full density ($\rho_s = 1$) it's necessary to realize compaction pressures about $9\sigma_s$ for copper powder A_1 (see Figure 6.12a) while for mixture A_4 compaction pressure is believed to have to be achieved infinity ∞.

Realization of shear compaction scheme (Figure 4.3 Modeling) enables to intensify a densification process. The increase of punches angle results in higher density of compacts (see Figure 6.12). As the experimental results show there are two main ways to increase compressibility of powder mixtures both in spraying and compaction processes:

- to decrease yield strength of powder particles, and
- to realize the shear compaction scheme.

From this viewpoint SIMAT spraying coating technique is more suitable because enables both to decrease yield strength of ductile powder and to enhance the action of shear stresses in thin layer being compacted due to high kinetic energy of spray stream.

6.2.2 The Rupture Strength of Compacted Powder Disks

The results of diametrical rupture strength determined by compression tests are shown in Figure 6.13.

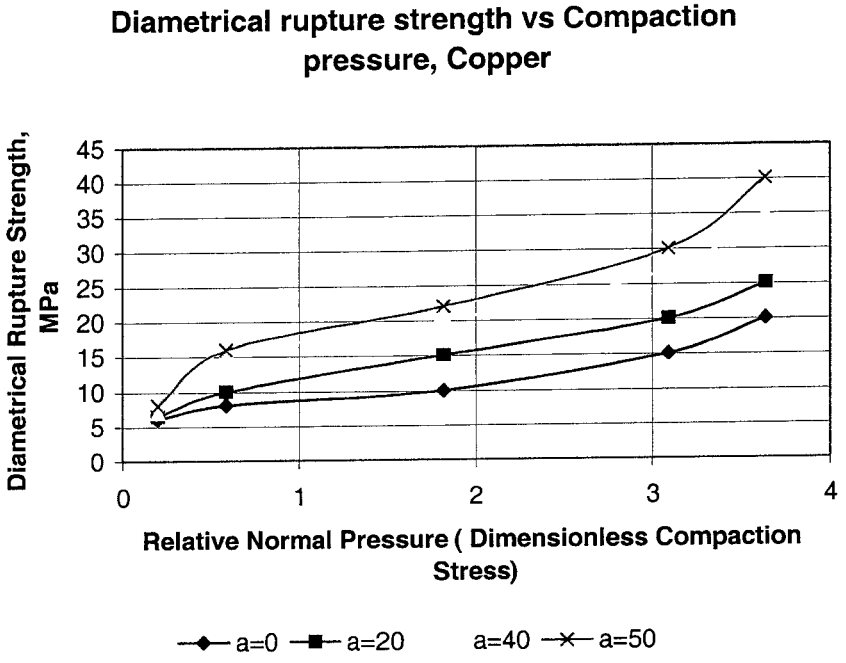
Diametrical rupture strength vs Compaction pressure, Copper
Diametrical Rupture Strength, MPa
45
40
35
30
25
20
15
10
5
0
0
1
2
3
4
Relative Normal Pressure (Dimensionless Compaction Stress)
a=0
a=20
a=40
a=50

a)

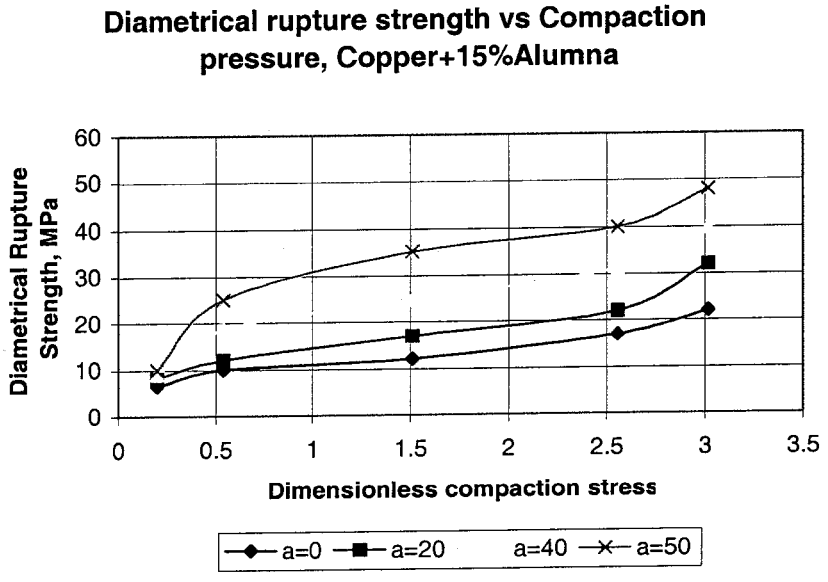
Diametrical rupture strength vs Compaction pressure, Copper+15%Alumna
Diametrical Rupture Strength, MPa
60
50
40
30
20
10
0
0
0.5
1
1.5
2
2.5
3
3.5
Dimensionless compaction stress
a=0
a=20
a=40
a=50

b)

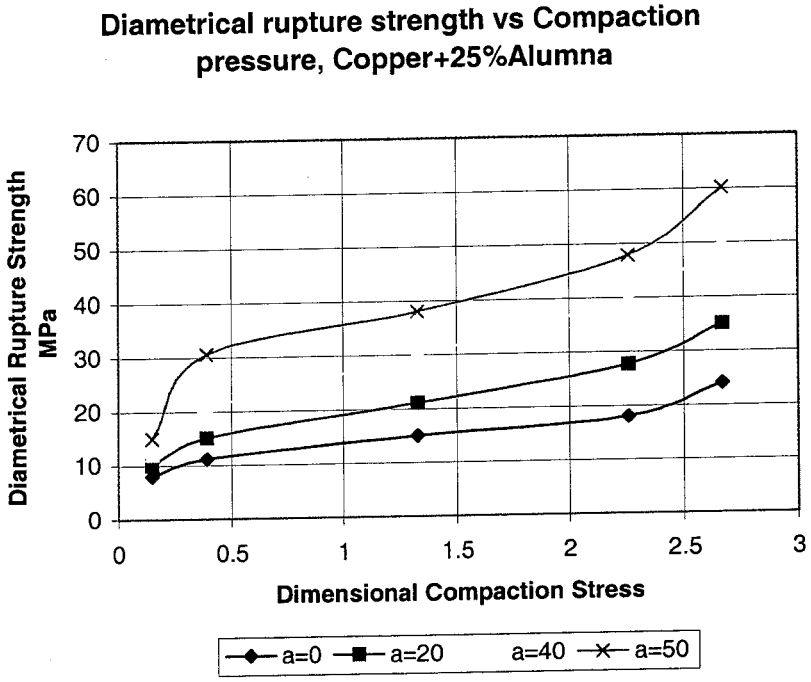

c)

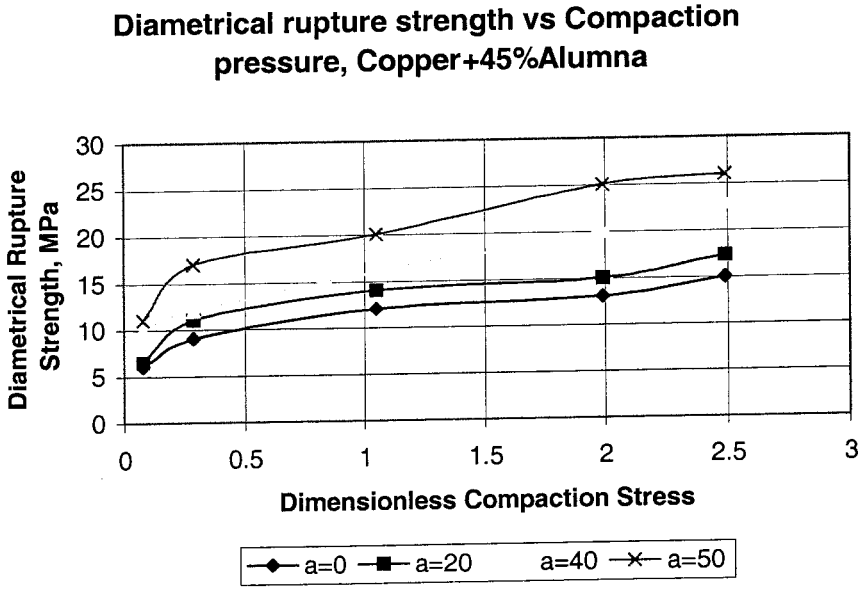

d)

Figure 6.13 **Dependences "diametrical rupture strength- dimensionless compaction normal stress" $\sigma_y = \sigma\ (\sigma_n / \sigma_s)$ for powder compacts of various compositions.**
a=0;20;40;50 – corresponds to punches angle $\varphi = 0^0; 20^0; 40^0; 50^0$.

These data shows a sharp sensitivity of rupture strength of powder compacts from compaction pressure and angle of punches especially for powder mixtures with high content of Alumna.

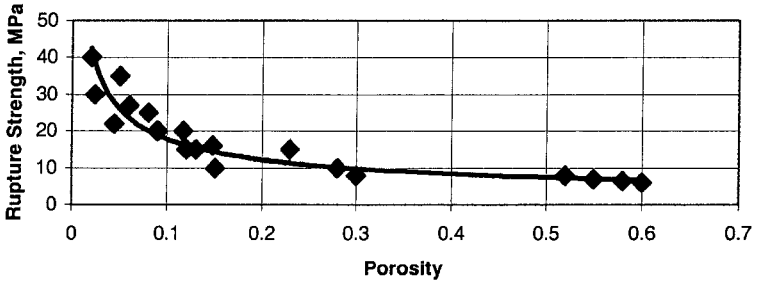

Figure 6.14 Failure Strength of Copper compacts

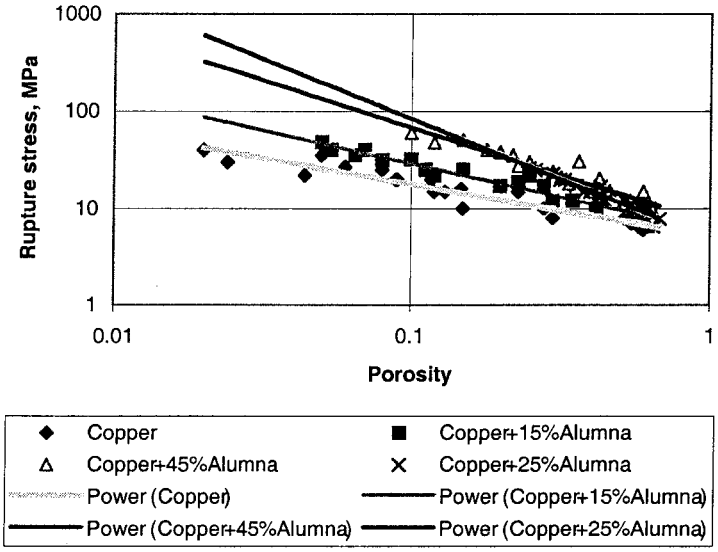

Figure 6.15 Failure Strength of Copper-Alumna compacts

An increase of Alumna content up to 25% rises the rupture strength. However for composition with 45% Alumna we received lower values of compact strength. Of course here we may see an effect of two factors : porosity and large strains of ductile powder particles during compaction process. So we plotted the graphs of function

$\sigma_y = \sigma\ (v)$ powder compacts studied (Figure 6.14 and 6.15). The data shown of Figures 6.15 reveals that the mechanical behavior of powder compacts is the same as for SIMAT sprayed layers. An approximation to high densities reveals clear that the strength of Copper + 25%Alumna compact is higher than Copper + 45%Alumna. The main reason of such effect is a creation of hard particle percolation network (see Figure 6.4).

6.3 Examination and Comparison of SIMAT Coating and Modeled Compacts Structure

One should note that in the case of Aluminum coatings microstructure examination is difficult to observe how the hard phase particles interact with Aluminum particles and estimate the distribution of pores in deposited composite. Analysis of microstructures shown on Figures 6.16 and 6.17 does not reveal strong difference between pores and Alumna particles at small magnifications.

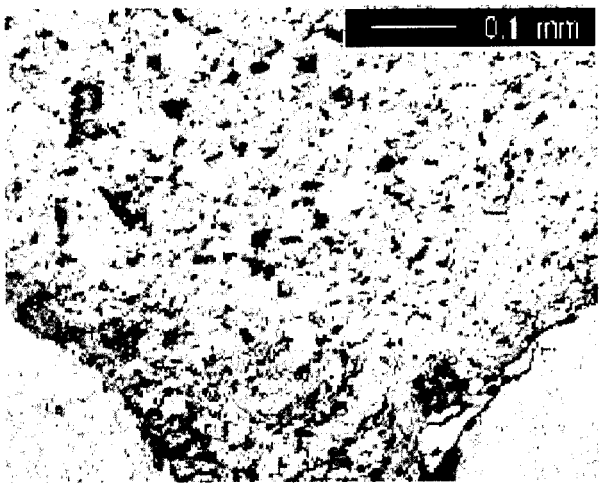

Figure 6.16 Microstructure of Al-Alumna coating (without etching ,x200)

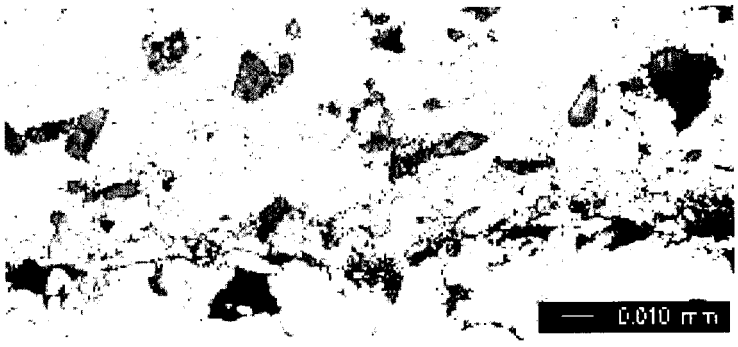

Figure 6.17 Microstructure of Al-Alumna coating (without etching ,x800)

At the same time on Figures 6.16 and 6.17 one can see a separate pores and hard phase particles but cannot observe an interparticle boundaries and location of both particles and pores because of examination of structures without etching.

Thus, the aims of structure examination of modeled compacts were :

1. to compare the structures of compacts with real coating structure
2. to observe the influence of hard phase incorporation into soft metal matrix under shear compaction stress state.

The Copper based compacts were processed because their etching was easy made. In order to observe an interparticle and grain boundaries an etching with the solution of composition $5gr.Fe_2O_3 + 30ml.HCl + 100ml.H_2O$ was done.

The microstructures of etched Copper sample are shown on Figures 6.18, 6.19, 6.20.

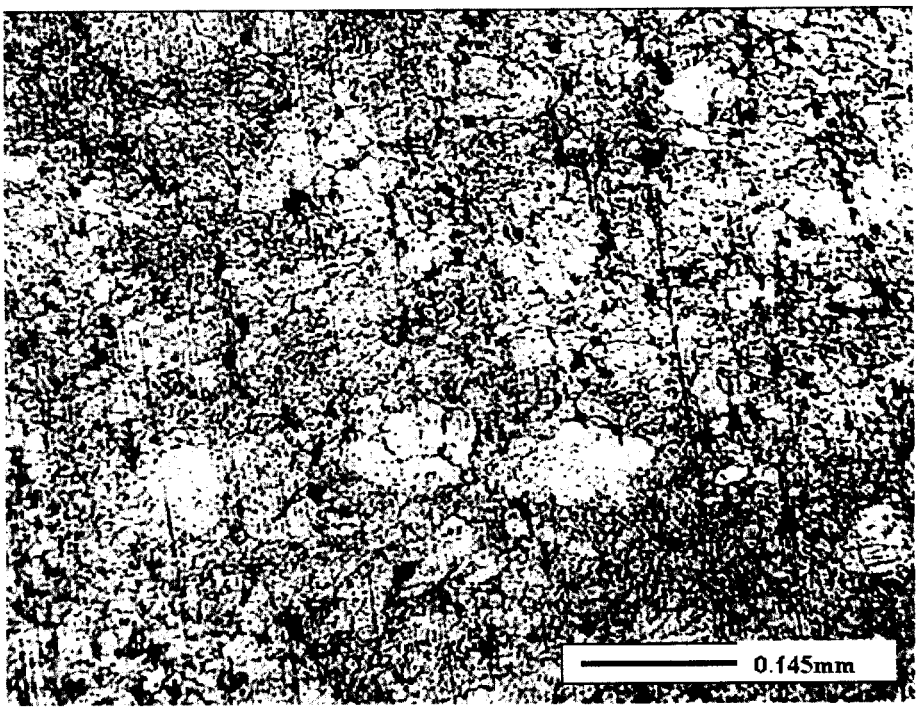

Figure 6.18 Microstructure of Copper compact after shear compression by 50^0 angle punches at Normal pressure 150MPa. (etching ,x220)

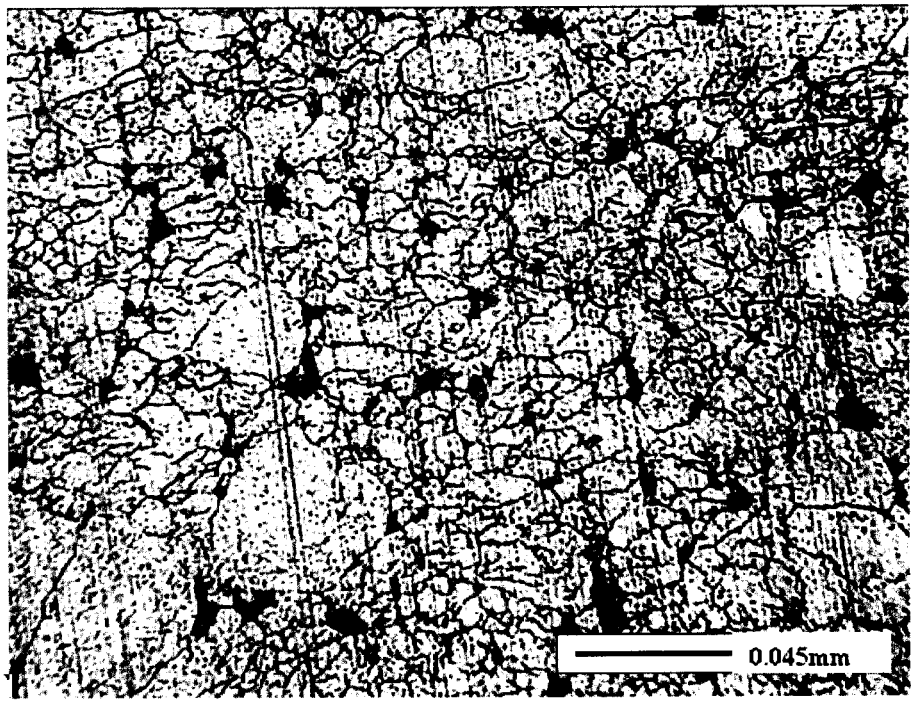

Figure 6.19 Microstructure of Copper compact after shear compression by 50^0 angle punches at Normal pressure 150MPa. (etching ,x880)

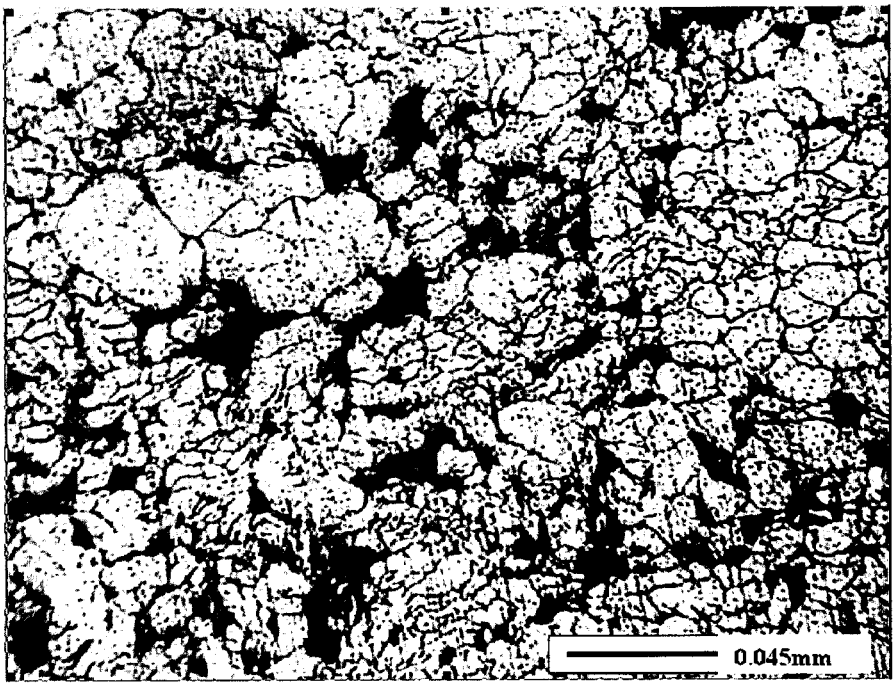

Figure 6.20 Microstructure of Copper compact after simple compression by 0^0 angle punches at Normal pressure 400MPa. (etching ,x880)

An observation of microstructure under small magnification does not ensure to exactly define the boundaries between particles in spite of etching (Figure 6.18) while analysis under higher magnification clearly shows that large quantity of small Copper particles form areas with high near full density due to large shear strains (Figure 6.20). At the same time simple compression without shears (punches' angle 0^0) with higher normal pressures results in high porosity and bigger sizes of pores (Figure 6.20) than for the shear scheme (Figure 6.19).

The results of microstrusture examination of Copper + Alumna compacts are shown on Figures 6.21 - 6.25. Firstly it is observed the consistency between real coating and modeled compact microstructures both for small (Figures 6.16 and 6.21, 6.22) and large magnifications (Figures 6.17, 6.18 and 6.23 – 6.25). However, it is difficult to separate the small particles of hard phase and pores under small magnification.

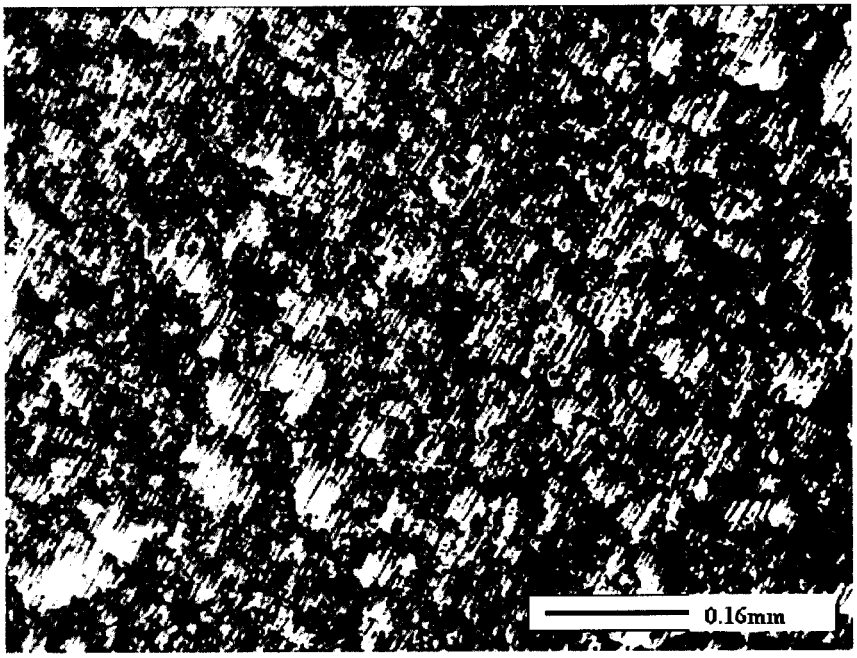

Figure 6.21 Microstructure of Copper+45%Al_2O_3 compact after shear compression by 50^0 angle punches at Normal pressure 150MPa. (etching ,x220)

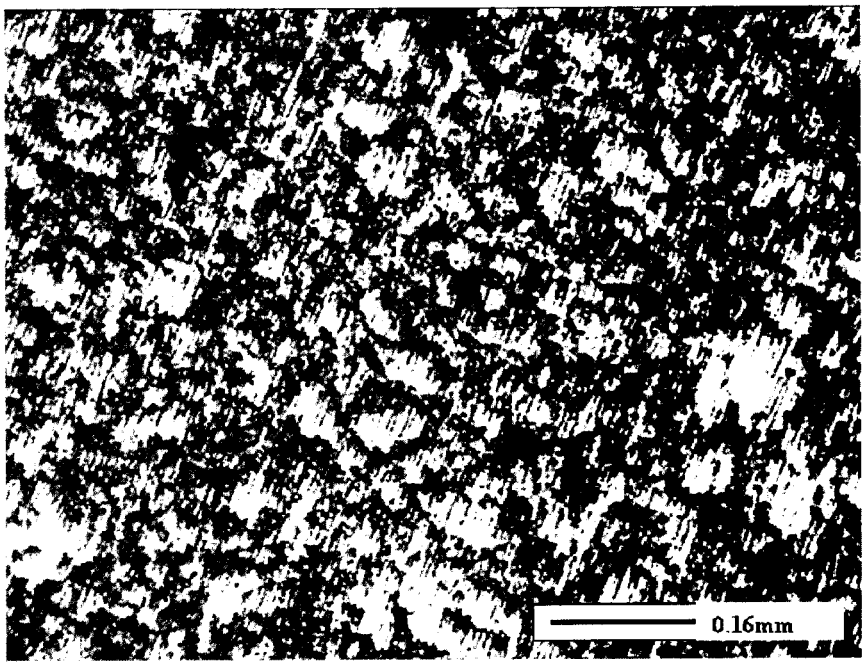

Figure 6.22 Microstructure of Copper+25%Al_2O_3 compact after shear compression by 50^0 angle punches at Normal pressure 150MPa. (etching ,x220)

A comparison microstructures (Figures 6.21, 6.22) reveals that decrease of hard phase content results in more uniform distribution of these particles and lower pore content . The compression of metal-hard particle mixtures results in penetration of hard particles into metal grains and formation of dense agglomerates (see, for example, Figure 6.24, red arrows) . The hard particles are located in the pore areas and in many cases assist to intensive plastic flow of soft metal particles. As a result, many of hard particles are locked by other metal powder particles that increase the strength of composite. It is obvious that the same processes occur during real SIMAT Spraying operation.

In order to more clearly observe the hard phase distribution in metal matrix the study of microstructure was performed on the mixtures Cu + SiC. So Alumina was replaced by Silicon Carbide with the same proportions because SiC may be clearly observed as a blue phase. So the the pores is observed as a dark areas, metal matrix particles – as a bright phase, and SiC – as a light blue phase (Figure 6.23, 6.24, 6.25).

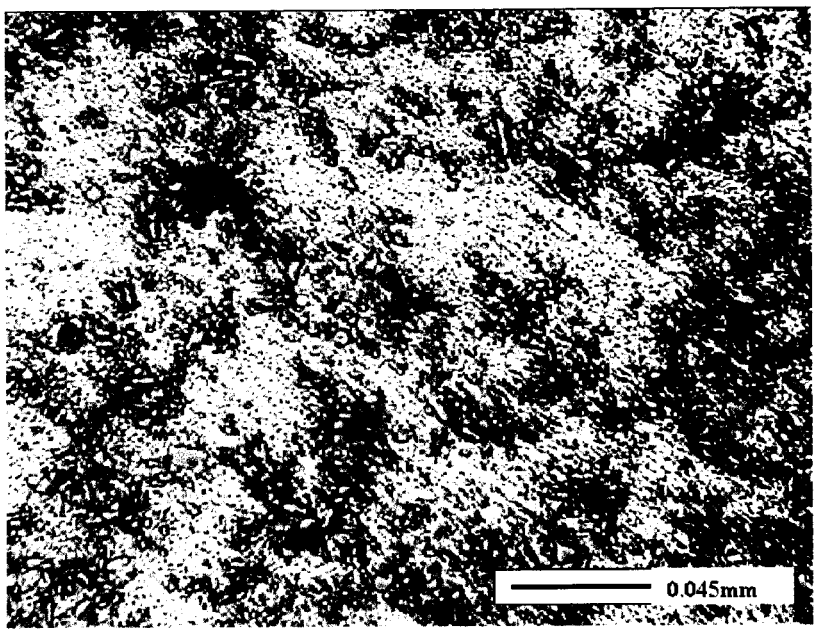

Figure 6.23 Microstructure of Copper+25%Al_2O_3 compact after shear compression by 50^0 angle punches at Normal pressure 100MPa. (etching ,x880)

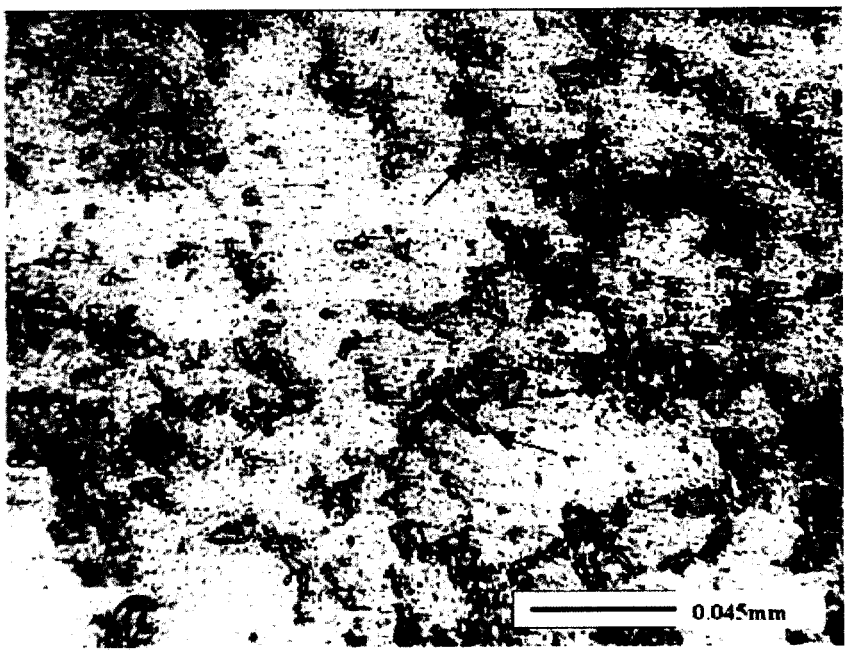

Figure 6.24 Microstructure of Copper+15%Al_2O_3 compact after shear compression by 50^0 angle punches at Normal pressure 150MPa. (etching ,x880)
Red arrows show the penetration of SiC particles into metal.

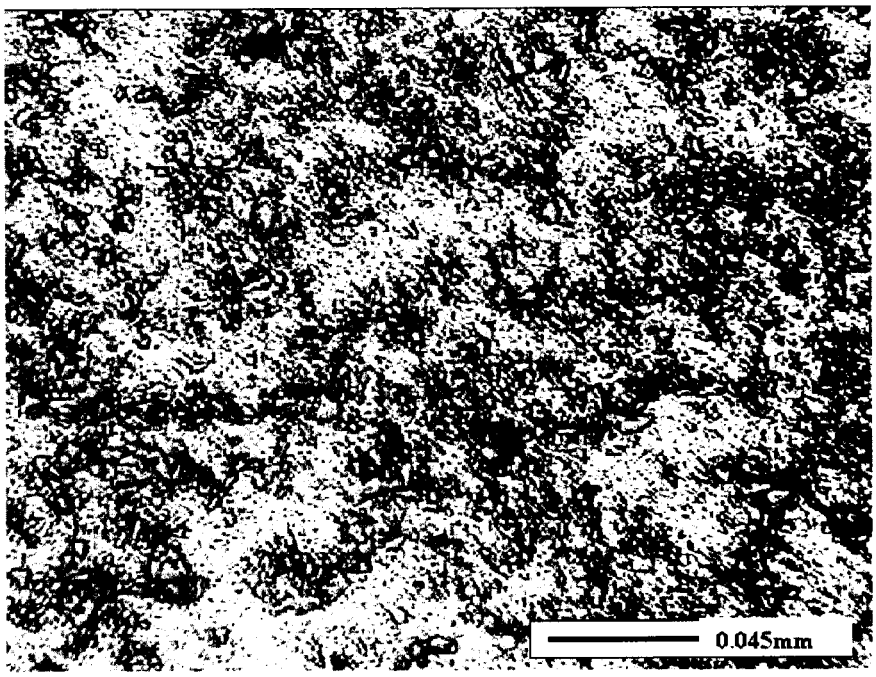

Figure 6.25 Microstructure of Copper+25%Al_2O_3 compact after shear compression by 50^0 angle punches at Normal pressure 200MPa. (etching ,x880)

Analysis of the hard phase content influence on the microstructure shows that increase of Al_2O_3 content up to 45% leads to formation of hard particles chains and agglomerates (Figure 6.21). This process impedes further densification of powder compact that results in higher porosity. Thus the concentration of hard phase has to be of near to percolation critical point ~30%.

Therefore the microstructure study of SIMAT coated and modeled compacts Show that the shear compression modeling ensures to properly determine the influence of hard phase content on the structure formation process and optimal concentration of hard particles in powder mixtures.

6.4 Comparison of Coating and Shear Compression Modeling results

A general comparison of SIMAT coating and Modeling experiments show that the main functions of porosity and mechanical properties of compacts and deposited layers are similar.

Shear Strain, γ	**SIMAT Spraying** Ultimate Tensile Strength (σ_{uts}), MPa			**Shear Compaction** Diametrical Failure Strength (σ_d), MPa		
	Cu	**Cu+15% Al_2O_3**	**Cu+25% Al_2O_3**	**Cu**	**Cu+ 15%Al_2O_3**	**Cu+ 25%Al_2O_3**
0	**50**	**60**	**62**	**14.2**	**18**	**22**
0.26	**71**	**85**	**89**	**19**	**25**	**32**
0.52	**89**	**121**	**127**	**27**	**37**	**45**
0.77	**98**	**142**	**151**	**29**	**43**	**55**
m **(σ_{uts} / σ_d)**	**0.28**	**0.3**	**0.36**			

Table 6.5 Comparison of Ultimate Strength of Copper Based Powder Compositions

The results of modeling as well as coating experiments show significant effect of stress-strain state of powder media on densification and interparticle interaction . Shear strains intensify these processes. This results in higher mechanical properties both coatings and compacts. The comparison of ultimate strength of samples made by two methods is shown in Table 6.5 These data reveals that relation $\boldsymbol{m = \sigma_{uts} / \sigma_d}$

(see Table 6.5) is approximately constant for each powder composition. This fact proves that shear compression modeling tests may be applied in order to determine optimal composition of powder mixtures to SIMAT Spraying Process and predict the behavior of powder mixtures in real SIMAT spraying.

Chapter 7

Advantages and Applications of the SIMAT™ Technology

7.1 Statement of impact and improvement over current technology

SIMAT™methodology enables material formation and deposition that is not fundamentally possible by any other known process. Thus, application and processing of coatings materials using SIMAT™ creates material options that are not currently possible.

The key advantages of SIMAT™ process are:

- High degree of coating material flexibility provided by low temperature deposition
- Large choice of coating materials
- High production spray rates
- Excellent, tenaciously bonded coatings
- Low oxide metallic coatings
- Dense with low porosity
- Very high coating thickness achievable
- Optimized microhardnesses
- Predictable coating chemistries
- Excellent machined surface finish
- Portability, ease to operate
- Easily integrated in various manufacturing processes.

7.2 SIMAT™ Application for Engine Production and Repair

All Copper and Aluminum based coatings used in the current development have been developed for engine built and repair applications. Aluminum based coatings have been used mostly for aluminum cylinder heads casting and corrosion pit repair when Copper based coatings have been used for cast iron casting repair on engine cylinder blocks. Both

types of coatings produce permanent material restoration and crack sealing that meet or exceed engine durability tests requirements. Below there is an example of the typical corrosion pit repair on an aluminum cylinder head.

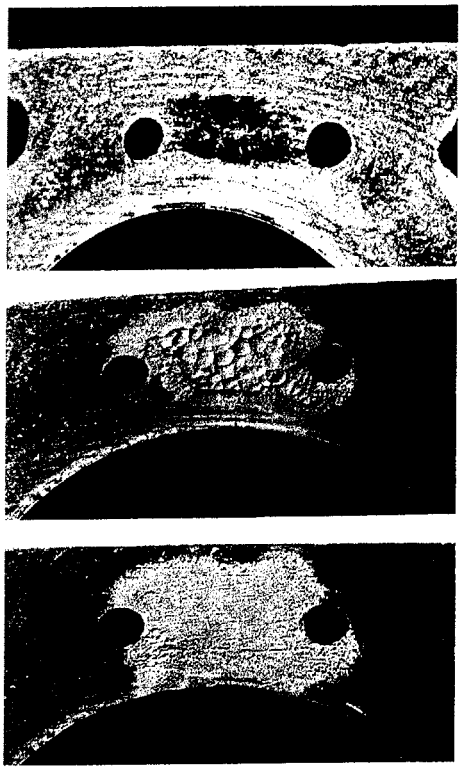

Figure 7.1 Illustration of SIMAT™ ability to repair corrosion damage in the head of a cylinder block that has conventionally irreparable pitting corrosion. Such repair and coating is possible on Steel, Aluminum, Copper and Titanium substrates. The process cost is also significantly lower than conventional spray technology.

The next level of SIMAT™ application for engine production is considered to be expanded to the area of sealing joints. This will possibly allow to exclude gaskets between major engine parts thus decreasing the number of engine components, overall weight and, consequently, costs. The SIMAT™ deposited materials proved to be dense and strong enough to withstand the load exerted on cylinder head gaskets, which is the weakest chain in the engine assembly right now. Meantime the same SIMAT™ material proved to provide sufficient flexibility necessary for hermetic sealing under high liquid or gas pressure. Corrosion resistance of the coatings contribute favorably to any major engine joint which is subject to thermal shock and aggressive gas and chemical liquid environment.

7.3 Potential SIMAT™ applications

Typical demonstrated applications of SIMAT™ process are:

- Fabrication of abrasion-resistant, corrosion-resistant, chemical attack-resistant and heat-resistant coatings on various parts
- Connection of units, hermetic sealing of tubing and reservoirs, stopping leakage, mechanical connection of parts and components made of different materials (e.g. ceramic-metal joints)
- Protection of steam turbine blades from cavitations wear
- Restoration of shapes and dimensions of moderately worn-out parts made of cast Aluminum, Copper, Bronze
- Fabrication of electro-conductive layers on ceramic materials.
- Fabrication of light-reflecting layers on glass
- Ornamental microerosive surface processing-to frost glass, to give a mat surface to ceramics, metals, etc.

A wide range of powder inorganic materials can be utilized for coating deposition (metals metal alloys, metal oxides, metal ceramic mechanical mixtures, ceramics, etc.). Typical materials that can be used in the SIMAT™ process include:

- Metals: Al, Ag, Cu, Zn, Ti, Ni, Fe
- Alloys: Cu-Al, Cu-Zn, Cu-Sn, Fe-Al, Ni-Ag, Brazing alloys
- Ceramics Al2O3, AlN, SiO2, SiC, TiN, ZrO2, etc.

One of the most innovative and demandable applications of SIMAT™ is its application in Tooling and Molding industries. Hard Facing operation delivered by SIMAT™ is believed to be applicable for on-line quick repair and tool surface restoration, however classical SIMAT™ powder mixtures are not useful in this particular case. It is necessary to move to area of complex steel alloys initially designated for Metal Powder Injection Molding and Thermal Spray applications and to find ways for their processing.

SIMAT™ is believed to be able to deliver Die Wall Lubricating Coatings leaving the die surface intact meantime significantly increasing the die production time. Especially this feature is important for Cold Stamping and Hydro Forming processes were lubricating coatings, besides their main designation, can control the blank material flow.

Thermal Barrier Coatings represent another potential scope of SIMAT™ application which related to Metal Casting and Forging. It is well known that the most harmful factors affecting die cavity surface life are temperature and erosion. If a suitable die surface thermal barrier coatings and application processes were developed, the potential cost savings would be great. The application of SIMAT™ is being considered as a potential solution method.

7.4 SIMAT™ Facility and Application Illustrations

The equipment to implement SIMAT™ can be developed and designed as a fixed automated manufacturing facility or a portable unit for flexible field applications. Early SIMAT™ units illustrated in pictures are available for testing and application development. The technology is applicable to very broad materials range and requires further application optimization. Elements of the SIMAT™ process are ready for industrial applications while many other advanced applications can be implemented by proper research and development.

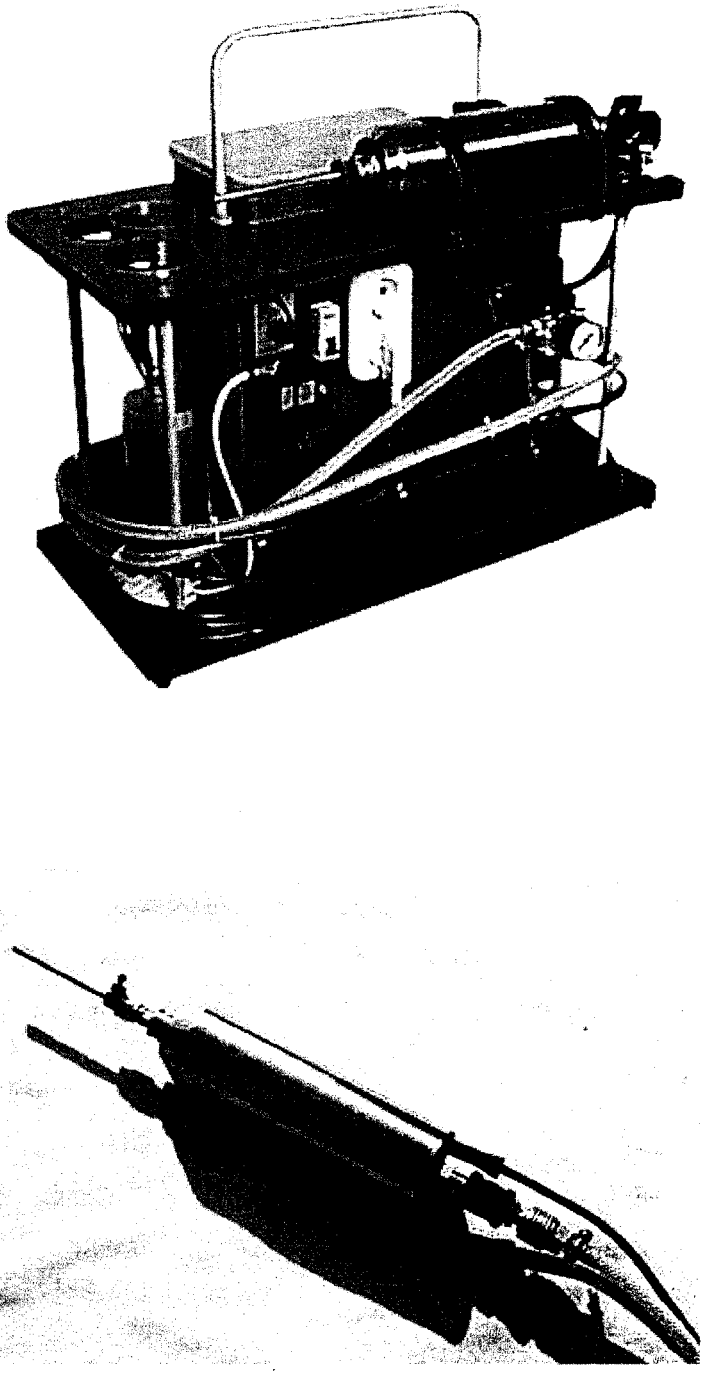

Figure 7.2 Portable SIMAT™ spraying apparatus and spraying gun used for the current development.

References

[1] **Budinski, Kenneth G.**, *Engineering Materials : Properties & Selection*, Prentice Hall, 1998, ISBN: 0139047158

[2] **Mark Smith**, *Materials World*, Vol. 9 no. 9, pp. 15-16, September 2001

[3] **A. Papyrin**, *A New Method for Coatings Deposition: New Generation of Technologies,* Five-page process description, Institute of Theoretical and Applied Mechanics, 1995

[4] **R. Gr. Maev**, *Supersonically Induced Mechanical Alloy Technology*, Centre For Imagine Research and Advanced Material Characterization, Canada, 2001

[5] **H. Kreye, T. Stoltenhoff,** *Cold Spraying - A Study of Process and Coating Characteristics*, Proc. of the 1st Intern. Thermal Spray Conference, ASM International USA, Montreal, Canada, 2000, p. 419-422

[6] **T. Stoltenhoff, H. Kreye, W. Kroemmer, H.J. Richter**, *Cold Spraying - from Thermal Spraying to High Kinetic Energy Spraying*, Proc. 5th HVOF Colloquium, Erding, 2000, GTS Ed., p 29-38

[7] **A. A. Shirzadi, H. Assadi, E. R. Wallach**, *Interface evolution and bond strength of diffusion bonding materials with stable oxide films, Surface and Interface Analysis*, Proc. of the 1st Intern. Thermal Spray Conference, ASM International USA, Montreal, Canada, 2000, p. 258-266

[8] **C. Borchers, T. Stoltenhoff, F. Gaertner, H. Kreye, H. Assadi and K. Krug,** *Deformation microstructure of cold sprayed coatings studied by electron microscopy*, Proceeding of MRS Spring Meeting, Boston, Massachusetts, April 2001

[9] **T. Stoltenhoff, H. Kreye, H. J. Richter, H. Assadi**, *Optimization of the cold spray process*, Proceeding of ITSC, Singapore, May 2001

[10] **A. Papyrin**, *Modeling of Particle-Substrate Adhesive Interaction Under the Cold Spray Process*, ITSC 2003 Technical Program (Abstract), Orlando, May, 2003

[11] **A. Papyrin**, *Cold Gas-Dynamic Spray Technology*, General Description, Ktech Technologies TSS Report, 2000

[12] **Tobias Schmidt**, *High strain rate deformation phenomena in Explosive Powder Compaction and Cold Spraying*, ITSC 2003 Technical Program (Abstract), Orlando, May, 2003

[13] **Delwyn L. Gilmore, Richard A. Neiser, Ronald C. Dykhuizen**, *Modeling the Critical Velocity for the Deposition in the Cold Spray Process*, Sandia National Laboratories Report, Albuquerque, NM, 2001

[14] **S. Shima, M. Oyane**, *Plasticity Theory for Porous Metals*, Material Science, June,1976, p 285-291

[15] **R.G. Green**, *Plasticity Theory for Porous Solids, Material Science*, April, 1972, p.109-120

[16] **V.M. Segal**, *A variant of plasticity theory for porous solids*, Applied Mechanics , Edition 17, 1981, p. 44-49

[17] **Frocht M. M.,** *Photoelasticity*, V 1, 2, J. Wiley, 1971

[18] **Seed G. M.,** *Strength of Materials,* An Undergraduate Tex, Saxe-Coburg Publ., Edinburgh, 2001, p. 544, ISBN 1-874-672-12-1

[19] *P/M self-lubricating bearings*, MPIF Standard 35, 1998

[20] *Porosity measurement*, MPIF Standard 42, 1999

[21] *Tensile test ASTM D638*, 1996

VITA AUCTORIS

NAME:	Evgeny Leshchinsky
PLACE OF BIRTH:	Lugansk, Ukraine
YEAR OF BIRTH:	1965
EDUCATION:	East Ukrainian University, Lugansk, Ukraine 1982 – 1990 M.A.Sc.
Canada	University of Windsor, Windsor, Ontario, 2000 – 2003 M.A.Sc.